Neutron imaging

Nikolay Kardjilov

HZB Helmholtz Zentrum Berlin

Oxford Neutron School 2024

Introduction

Free neutrons have high penetration power.

They are able to penetrate matter of relevant thickness (several µm to dm).

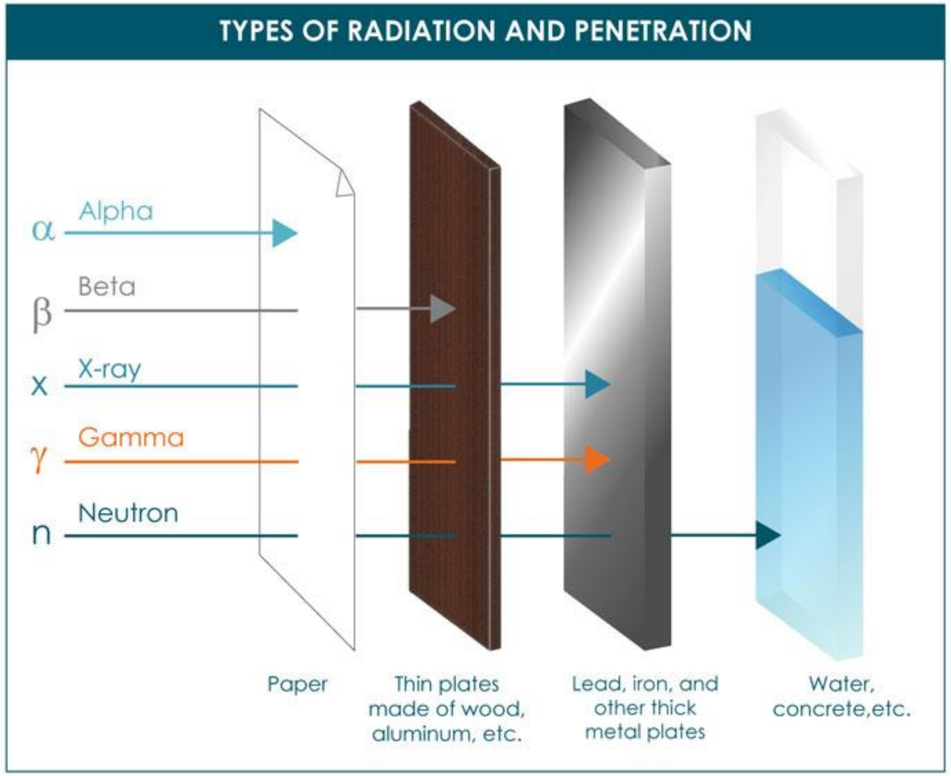

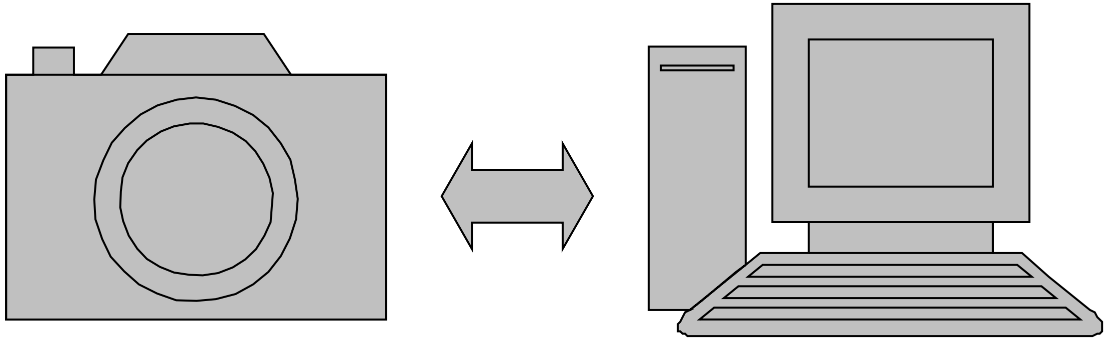

https://www.mirion.com/learning-center/radiation-safety-basics/types-of-ionizing-radiation

Attenuation contrast

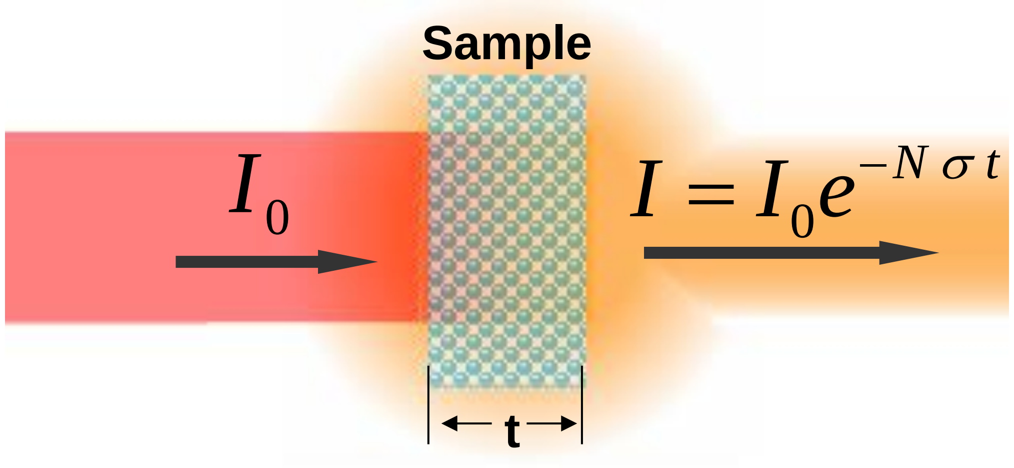

- N – numerical density of sample atoms per cm^3
- I_0 - incident neutrons per second per cm^2
- σ - neutron cross section in ~ 10^{-24} cm^2
- t - sample thickness

Transmission
(Beer-Lambert's law)

$$T = \frac{I}{I_0} = e^{-\Sigma * d} = e^{-\sigma * \frac{A}{M} * \rho}$$

and inverted …

$$\Sigma * d = \ln\left(\frac{I_0}{I}\right)$$

↙ ↘

Thickness d can be obtained when Σ is known	Density or composition derived if thickness d is known

Transmission image

- Neutrons can be detected with suitable devices (neutron imaging detectors)
- The distribution of the neutrons without a sample (unperturbed, «open» beam) $\boldsymbol{I_0}$ and after interaction within the sample $\boldsymbol{I}$ are measured.

- The ratio of the two images gives the neutron transmission in the beam direction *T(i,j)*

$$T = \frac{I}{I_0} = e^{-\Sigma * d}$$

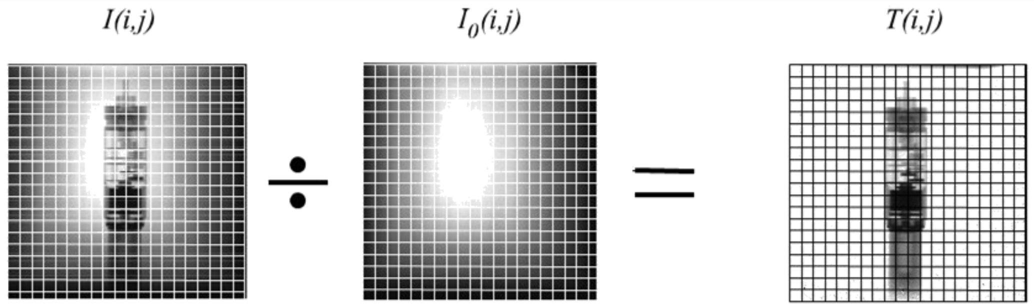

https://www.physics.nist.gov/MajResFac/NIF/radiography.html

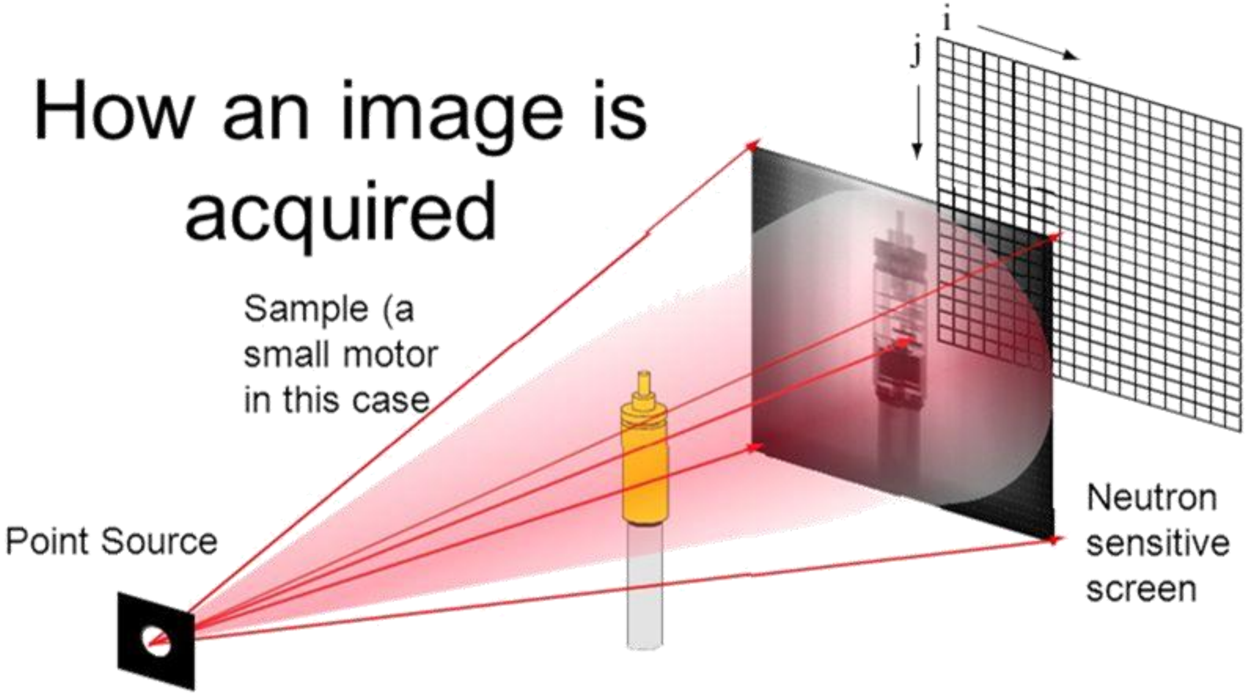

Transmission image

- Neutrons can be detected with suitable devices (neutron imaging detectors)
- The distribution of the neutrons without a sample (unperturbed, «open» beam) $\boldsymbol{I_0}$ and after interaction within the sample ***I*** are measured.

- The ratio of the two images gives the neutron transmission in the beam direction *T(i,j)*

$$T = \frac{I}{I_0} = e^{-\Sigma * d}$$

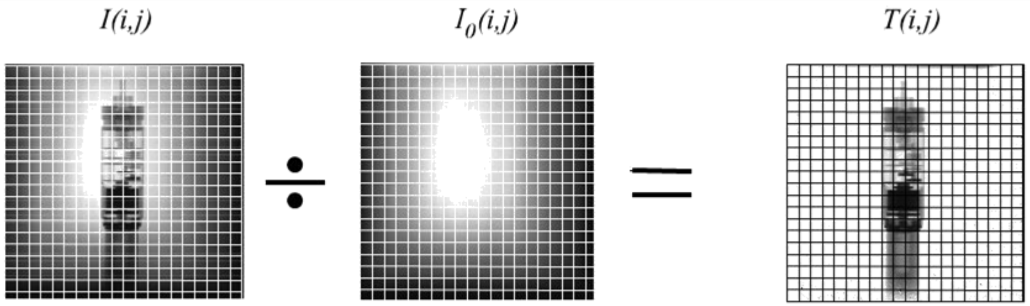

https://www.physics.nist.gov/MajResFac/NIF/radiography.html

Complementary X/N imaging

X-rays

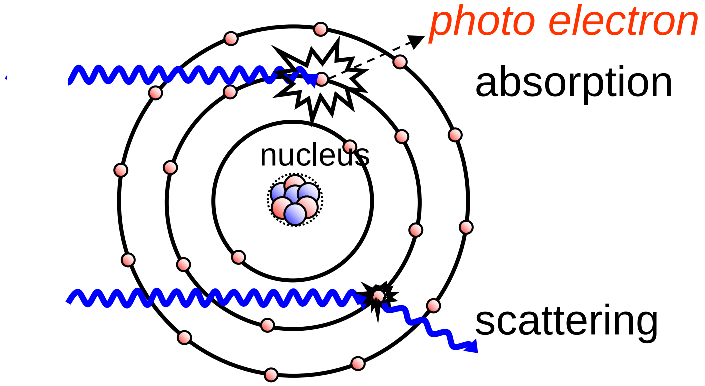

Attenuation coefficients with X-ray [cm?^{1}]

1a	2a	3b	4b	5b	6b	7b	8			1b	2b	3a	4a	5a	6a	7a	0
H 0.02																	He 0.02
Li 0.06	Be 0.22											B 0.28	C 0.27	N 0.11	O 0.16	F 0.14	Ne 0.17
Na 0.13	Mg 0.24											Al 0.38	Si 0.33	P 0.25	S 0.30	Cl 0.23	Ar 0.20
K 0.14	Ca 0.26	Sc 0.48	Ti 0.73	V 1.04	Cr 1.29	Mn 1.32	Fe 1.57	Co 1.78	Ni 1.96	Cu 1.97	Zn 1.64	Ga 1.42	Ge 1.33	As 1.50	Se 1.23	Br 0.90	Kr 0.73
Rb 0.47	Sr 0.86	Y 1.61	Zr 2.47	Nb 3.43	Mo 4.29	Tc 5.06	Ru 5.71	Rh 6.08	Pd 6.13	Ag 5.67	Cd 4.84	In 4.31	Sn 3.98	Sb 4.28	Te 4.06	I 3.45	Xe 2.53
Cs 1.42	Ba 2.73	La 5.04	Hf 19.70	Ta 25.47	W 30.49	Re 34.47	Os 37.92	Ir 39.01	Pt 38.61	Au 35.94	Hg 25.88	Tl 23.23	Pb 22.81	Bi 20.28	Po 20.22	At	Rn 9.77
Fr	Ra 11.80	Ac 24.47	Rf	Ha													
Lanthanides	Ce 5.79	Pr 6.23	Nd 6.46	Pm 7.33	Sm 7.68	Eu 5.66	Gd 8.69	Tb 9.46	Dy 10.17	Ho 10.91	Er 11.70	Tm 12.49	Yb 9.32	Lu 14.07			
*Actinides	Th 28.95	Pa 39.65	U 49.08	Np	Pu	Am	Cm	Bk	Vf	Es	Fm	Md	No	Lr x-ray			

neutrons

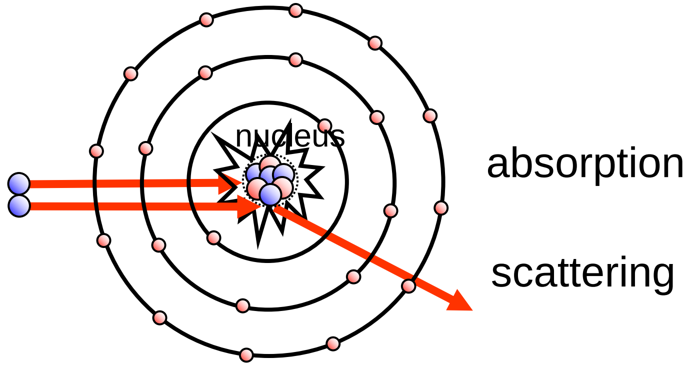

D 0.40

Attenuation coefficients with neutrons [cm?^{1}]

1a	2a	3b	4b	5b	6b	7b	8			1b	2b	3a	4a	5a	6a	7a	0
H 3.44																	He 0.02
Li 3.30	Be 0.79											B 101.60	C 0.56	N 0.43	O 0.17	F 0.20	Ne 0.10
Na 0.09	Mg 0.15											Al 0.10	Si 0.11	P 0.12	S 0.06	Cl 1.33	Ar 0.03
K 0.06	Ca 0.08	Sc 2.00	Ti 0.60	V 0.72	Cr 0.54	Mn 1.21	Fe 1.19	Co 3.92	Ni 2.05	Cu 1.07	Zn 0.35	Ga 0.49	Ge 0.47	As 0.67	Se 0.73	Br 0.24	Kr 0.61
Rb 0.08	Sr 0.14	Y 0.27	Zr 0.29	Nb 0.40	Mo 0.52	Tc 1.76	Ru 0.58	Rh 10.88	Pd 0.78	Ag 4.04	Cd 115.11	In 7.58	Sn 0.21	Sb 0.30	Te 0.25	I 0.23	Xe 0.43
Cs 0.29	Ba 0.07	La 0.52	Hf 4.99	Ta 1.49	W 1.47	Re 6.85	Os 2.24	Ir 30.46	Pt 1.46	Au 6.23	Hg 16.21	Tl 0.47	Pb 0.38	Bi 0.27	Po	At	Rn
Fr	Ra 0.34	Ac	Rf	Ha													
*Lanthanides	Ce 0.14	Pr 0.41	Nd 1.87	Pm 5.72	Sm 171.47	Eu 94.58	Gd 1479.04	Tb 0.93	Dy 32.42	Ho 2.25	Er 5.48	Tm 3.53	Yb 1.40	Lu 2.75			
**Actinides	Th 0.59	Pa 8.46	U 0.82	Np 9.80	Pu 50.20	Am 2.86	Cm	Bk	Cf	Es	Fm	Md	No	Lr neut.			

Complementary X/N imaging

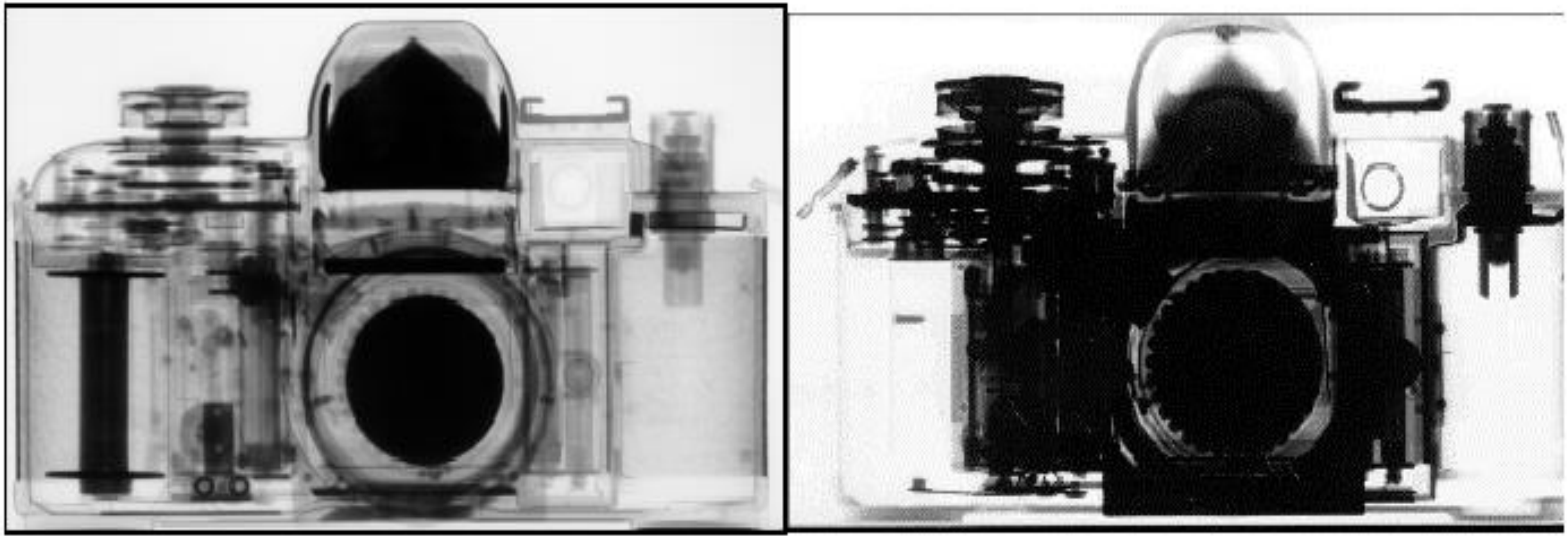

Complementary radiography of a camera using neutrons (left) and X-rays (right). Whereas the hydrogen containing parts can be visualised with neutron even at thin layers, thicker metallic components are hard to penetrate with X-rays.

Images courtesy: Dr. Eberhard Lehmann (Paul-Scherrer-Institute, Switzerland)

Beam collimation

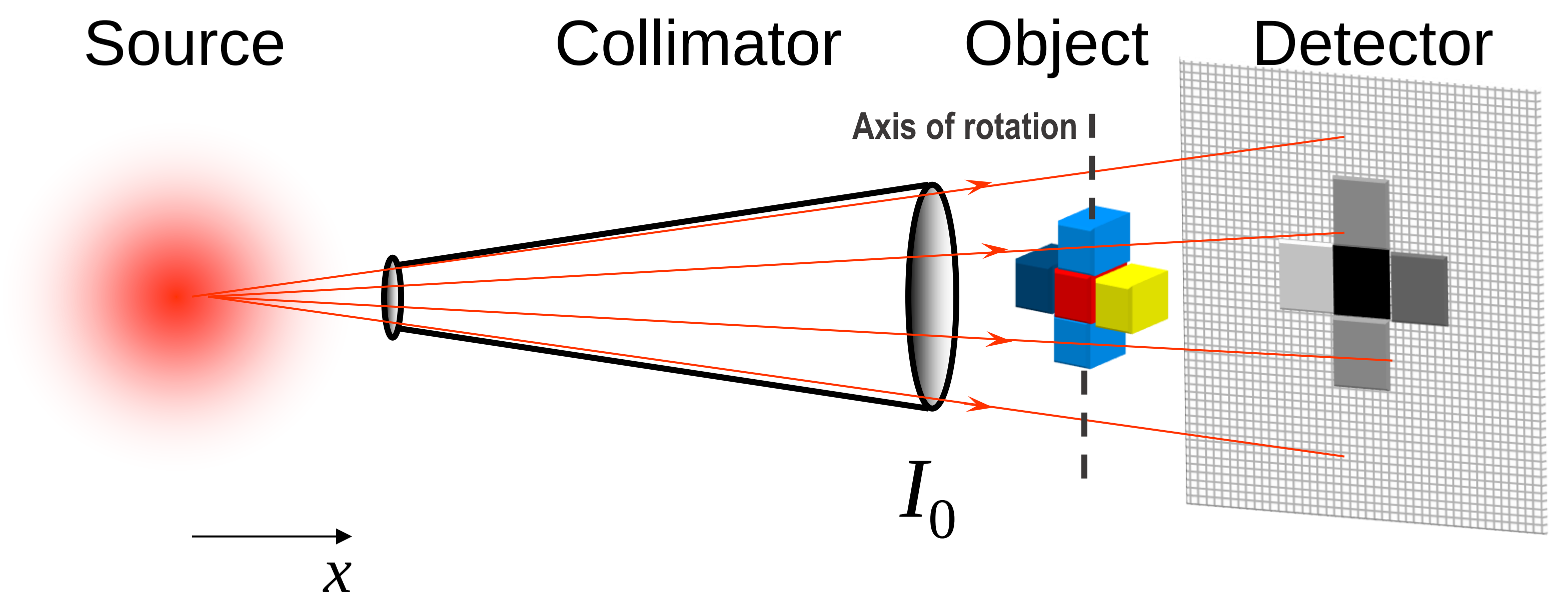

$$\sim I_0 e^{-\int \Sigma(x)dx}$$

x – propagation direction

I_0 – primary beam

$\Sigma(x)$ – attenuation coefficient

N. Kardjilov, et al. *Materials Today* 14.6 (2011): 248-256

HZB Helmholtz Zentrum Berlin

Beam collimation

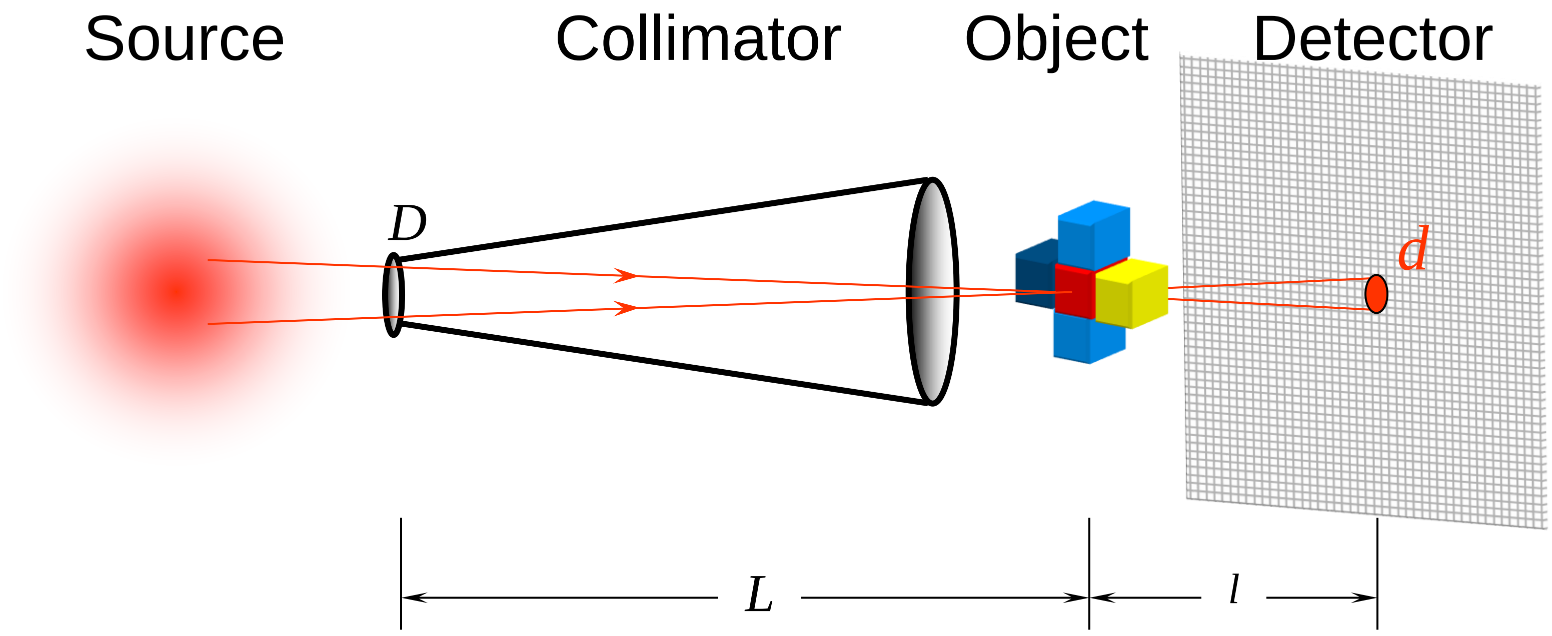

D – Collimator aperture
L – Distance Collimator-Object
l – Distance Object-Detector

$$d = \frac{l}{L/D}$$

The image sharpness (resolution) depends on the distance between sample and detector ***l*** and the beam collimation determined by the ratio ***L/D***.

Beam collimation

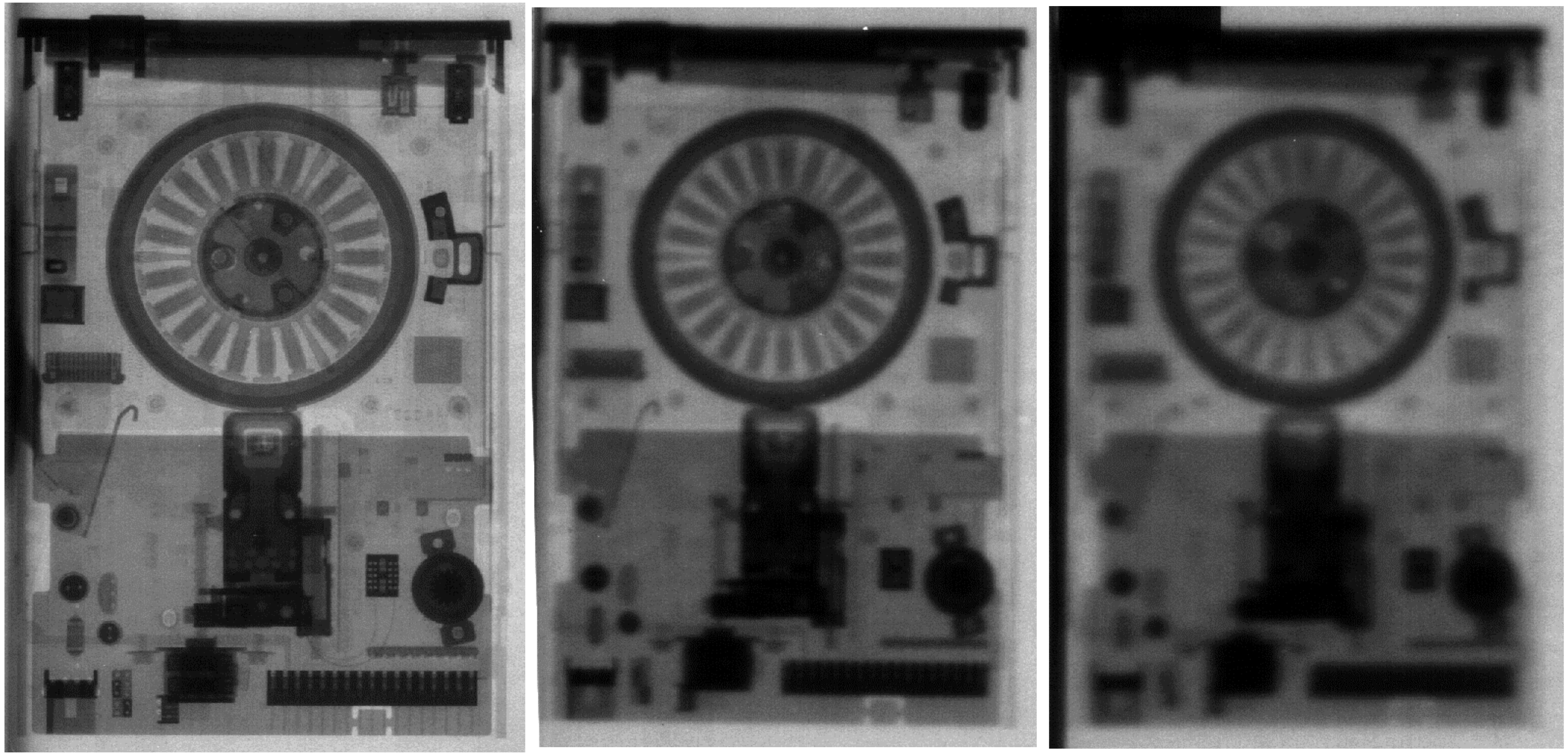

Radiographs of a 3,5" floppy drive in 0 cm, 10 cm and 20 cm distance from a film + Gd sandwich taken at a cold neutron guide with *L/D*=71.

B. Schillinger, Estimation and measurement of L/D on a cold and thermal neutron guide, in: Nondestructive Testing and Evaluation, World Conference on Neutron Radiography, vol. 16, Osaka, 1999, pp. 141–150

Design of neutron imaging instrument

Cold neutrons

Wavelength range: 1.5 Å – 10 Å

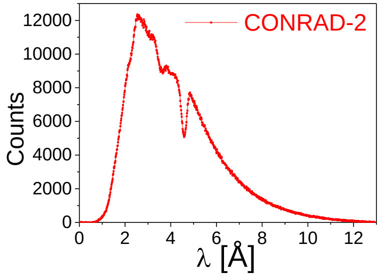

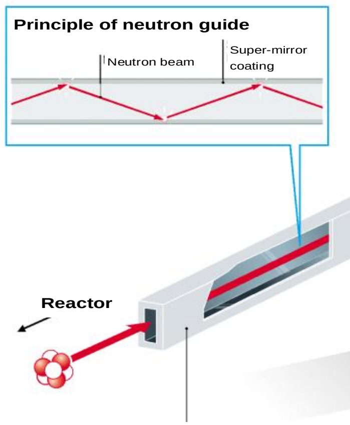
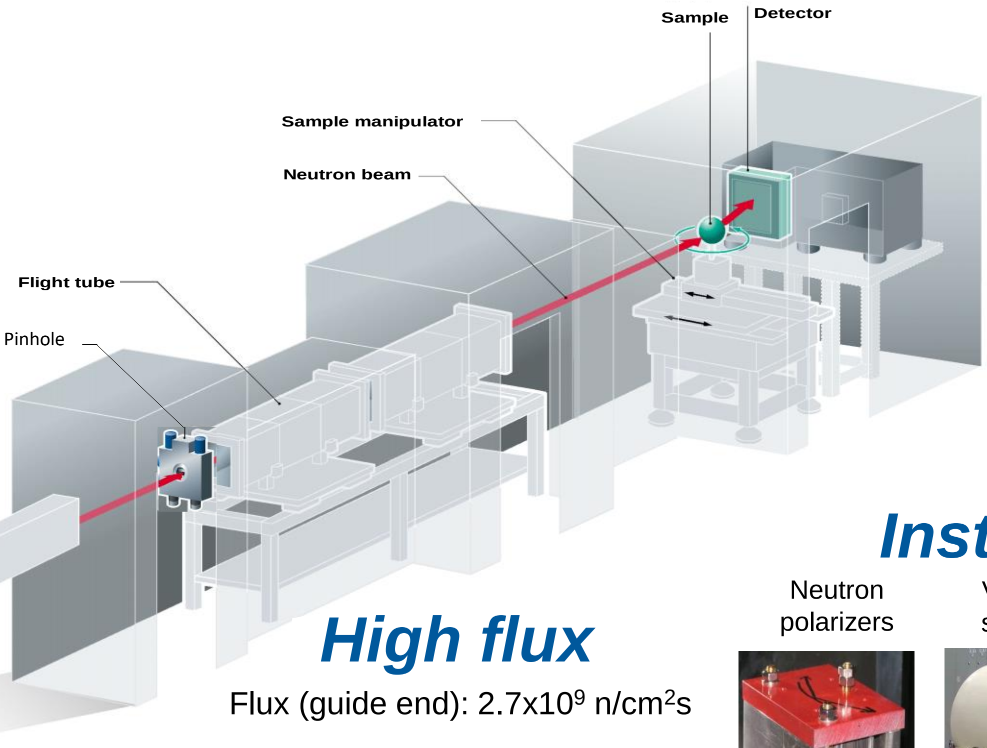

Guide system: super-mirror coated neutron guide (M=3) with a curvature of 750 m and length of 15 m followed by linear guide section (M=2) with a length of 10 m.

High flux

Flux (guide end): 2.7×10^9 n/cm^{2}s

Large beam

Beam size: 20 cm x 20 cm

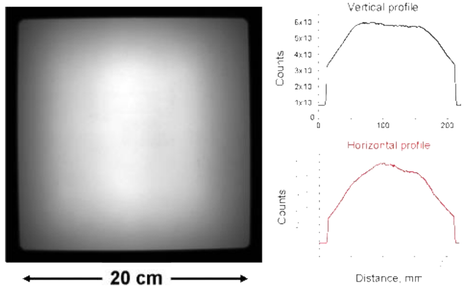

Instrumentation

Neutron polarizers

Velocity selector

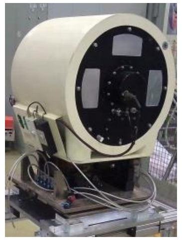

Double-crystal monochromator

Grating interferometry

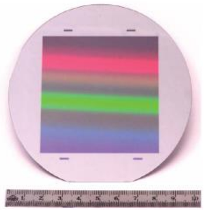

Neutron imaging detector

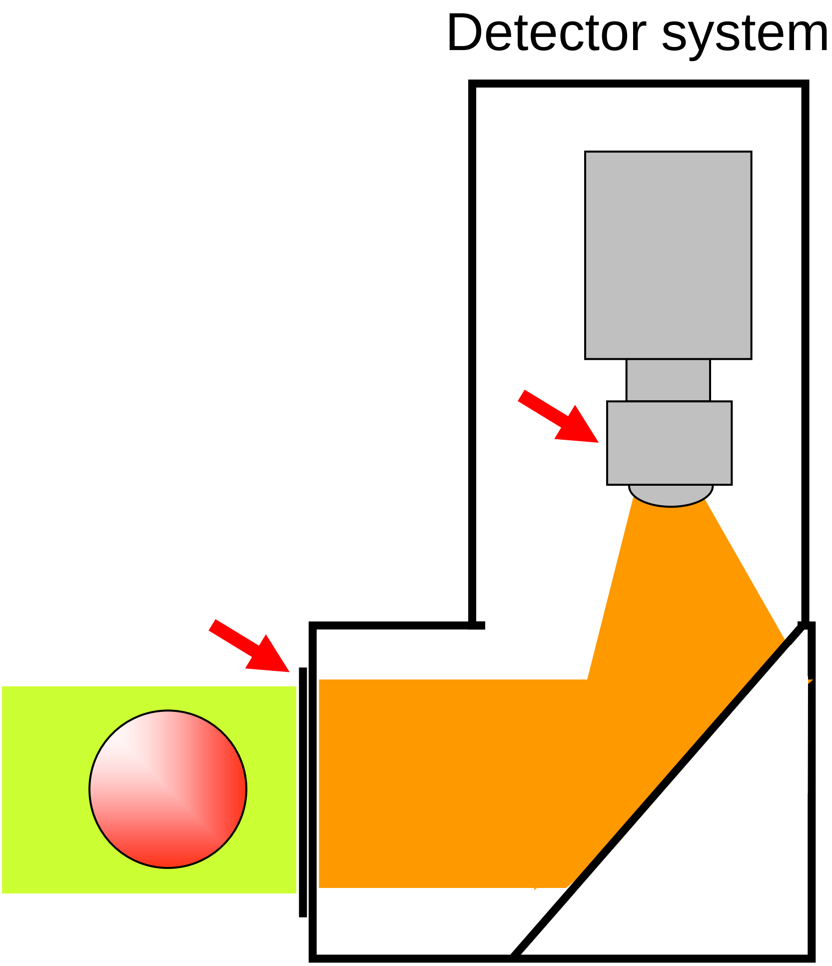

Standard setup

Scintillator: 200 µm 6LiF
Lens system: 50 mm
Pixel size: 100 µm
Exposure time: 20 s

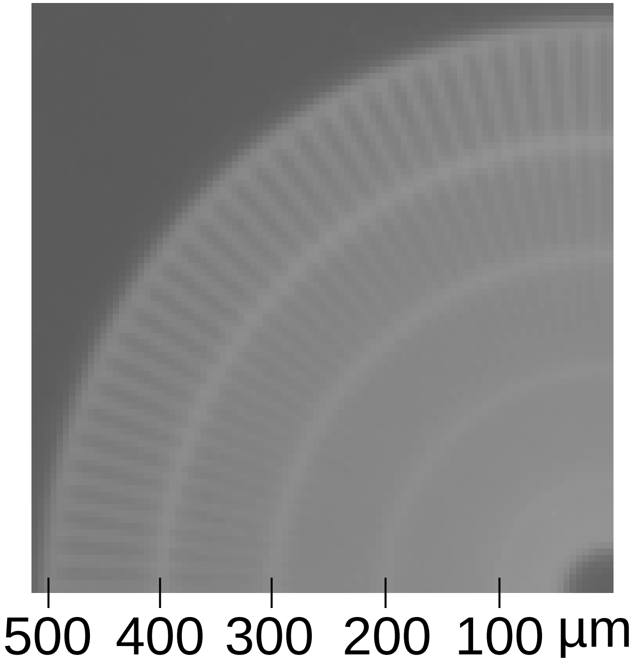

Neutron imaging detector

The ZnS+^{6}LiF scintillation screen is the limit of resolution.

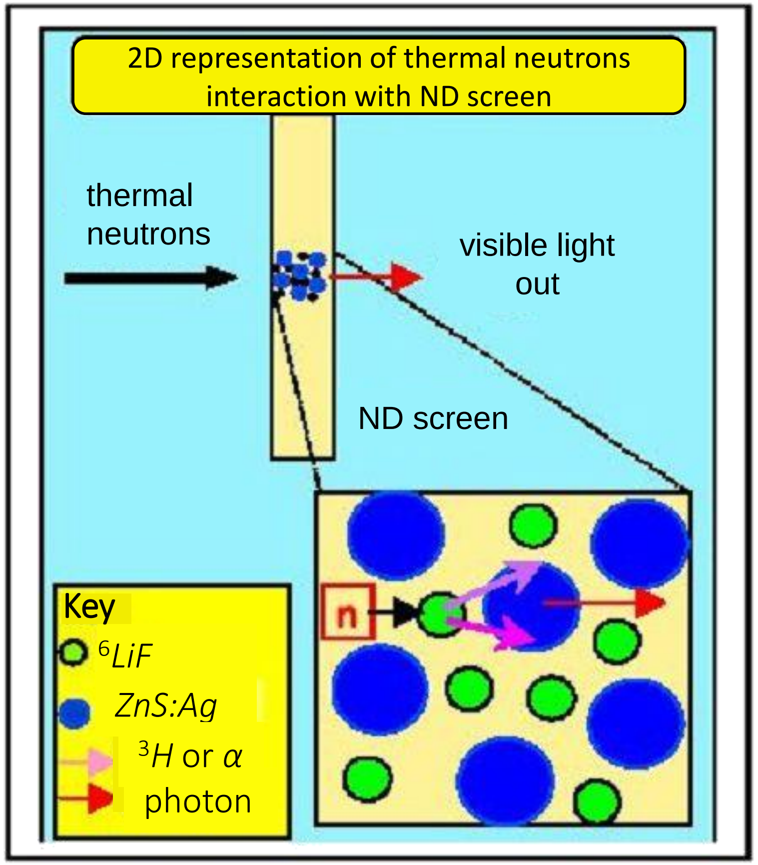

The reaction products of

$^6Li(n,\alpha) \rightarrow ^3H + ^4He + 4.7$ MeV

have to be stopped in the ZnS scintillation screen.
Their average range is in the order of 50-80 μm.

About 177,000 photons are generated per detected neutron.

With thinned scintillation screens, we can achieve resolution in the order of 20-30 μm.

Slide courtesy: Dr. Burkhard Schillinger (FRM-II, Munich, Germany)

Neutron imaging detector

Capture reactions for thermal / cold neutrons

$^{3}He + {}^{1}n \Rightarrow {}^{3}He + {}^{1}p + 0.77\ MeV$

→ $^{6}Li + {}^{1}n \Rightarrow {}^{3}H + {}^{4}He + 4.79\ MeV$

$^{10}B + {}^{1}n \Rightarrow {}^{7}Li + {}^{4}He + 2.78\ MeV \quad (7\%)$

$\Rightarrow {}^{7}Li^{*} + {}^{4}He + 2.30\ MeV \quad (93\%)$

$^{155}Gd + {}^{1}n \Rightarrow {}^{156}Gd + \gamma\text{´s} + \text{CE´s}\ (7.9\ MeV)$

→

$^{157}Gd + {}^{1}n \Rightarrow {}^{158}Gd + \gamma\text{´s} + \text{CE´s}\ (8.5\ MeV)$

$^{235}U,\ {}^{239}Pu\ {}^{1}n \Rightarrow$ fission products + 80 MeV

Neutron imaging detector

Scintillators, effect of thickness

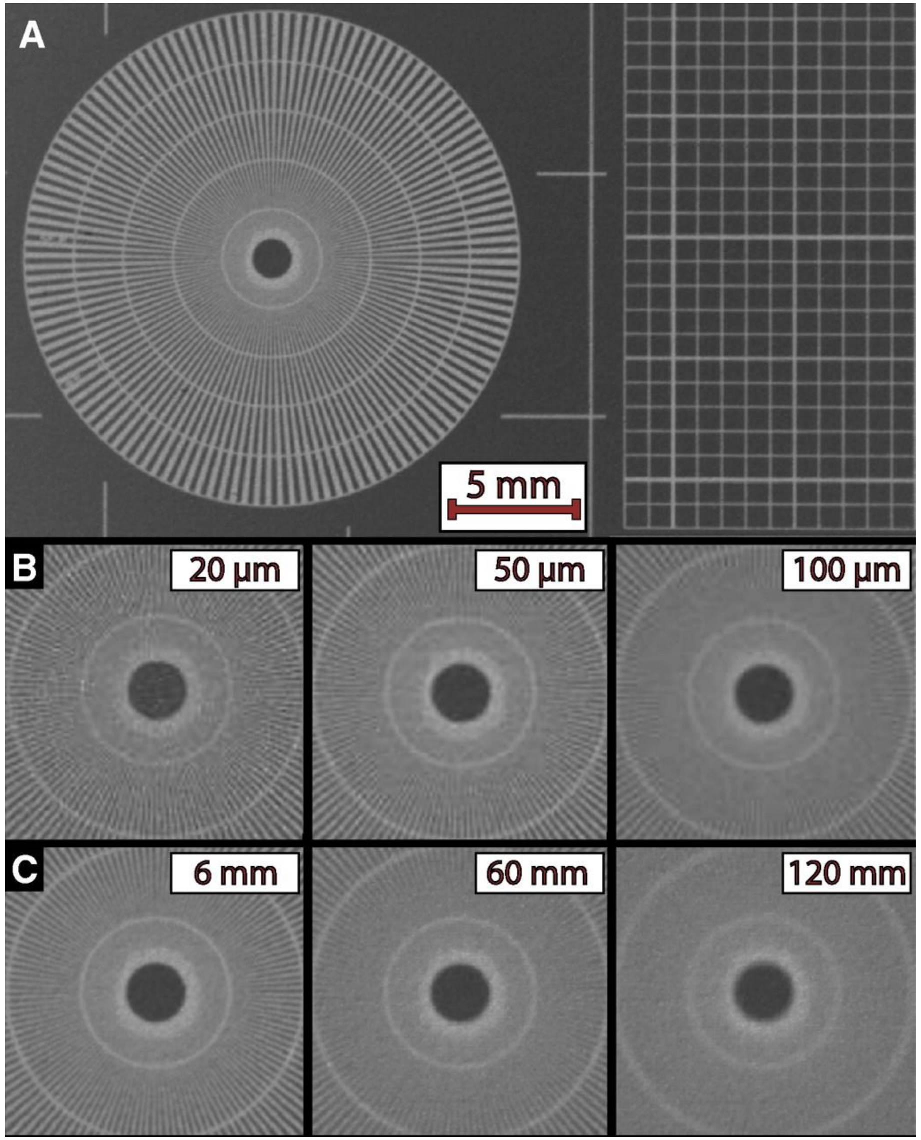

(A) A radiograph of the Siemens star test pattern used to study the effect of scintillator thickness, exposure time, and impact of geometrical blurring.

(B) Images showing the center of the Siemens star for scintillators of different thicknesses.

(C) The same region imaged by a scintillator of 50 µm thickness. In each image the test pattern is placed further away from the scintillator, resulting in increased geometrical blurring.

K.-U. Hess et al., Advances in high-resolution neutron computed tomography: Adapted to the earth sciences , Geosphere (2011) 7 (6): 1294-1302.

Tomography

Principle

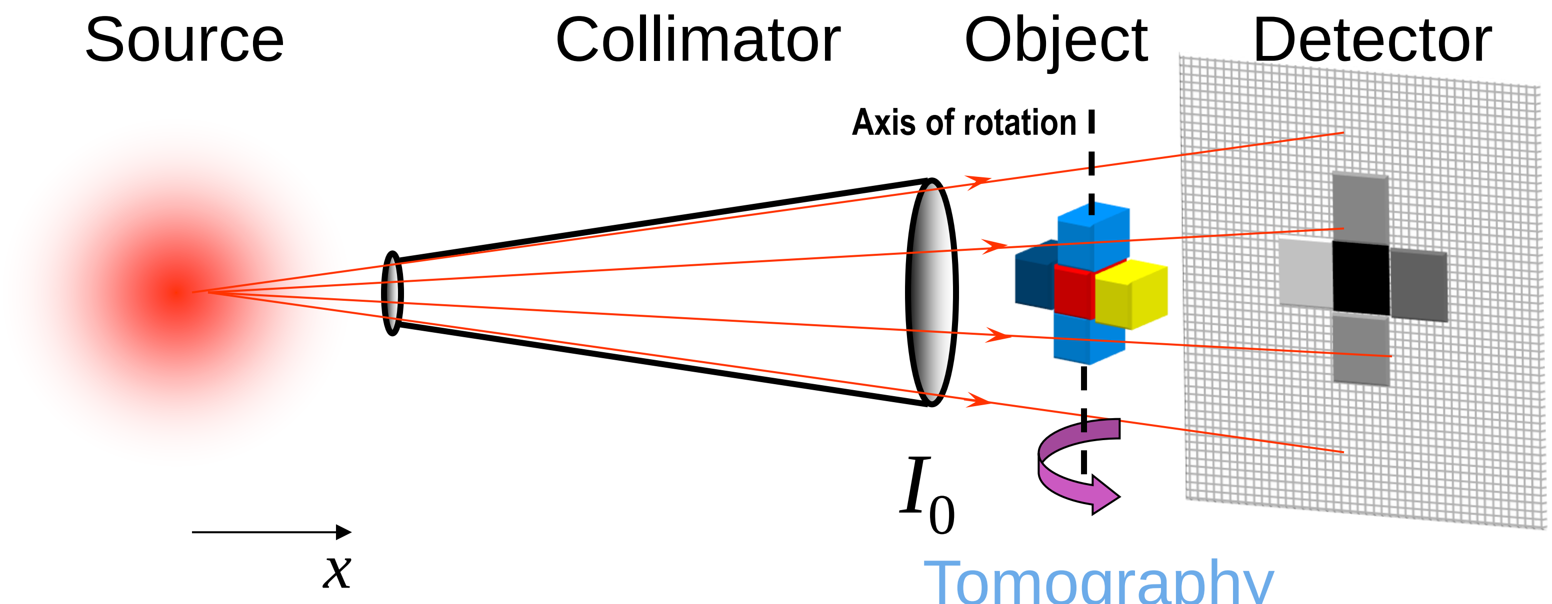

Tomography

$$\sim I_0 e^{-\int \Sigma(x)dx}$$

x – propagation direction

I_0 – primary beam

$\Sigma(x)$ – attenuation coefficient

N. Kardjilov, et al. *Materials Today* 14.6 (2011): 248-256

Tomography

Example: Stop watch

Angular projections:

Tomographic reconstruction:

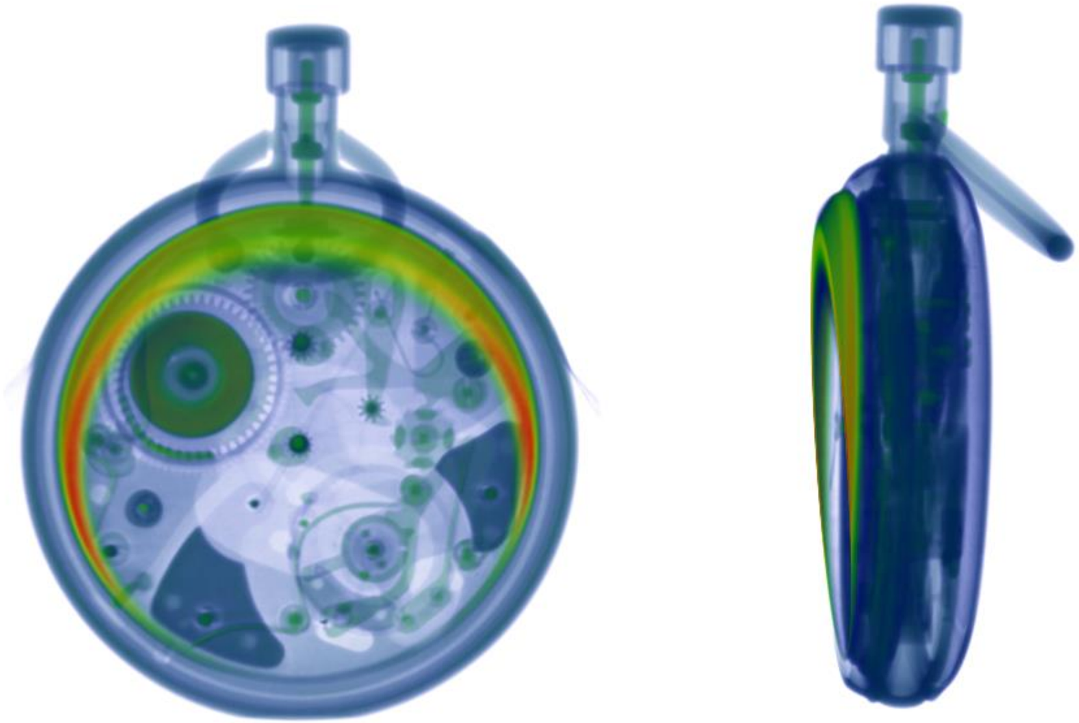

Tomography

Backprojection

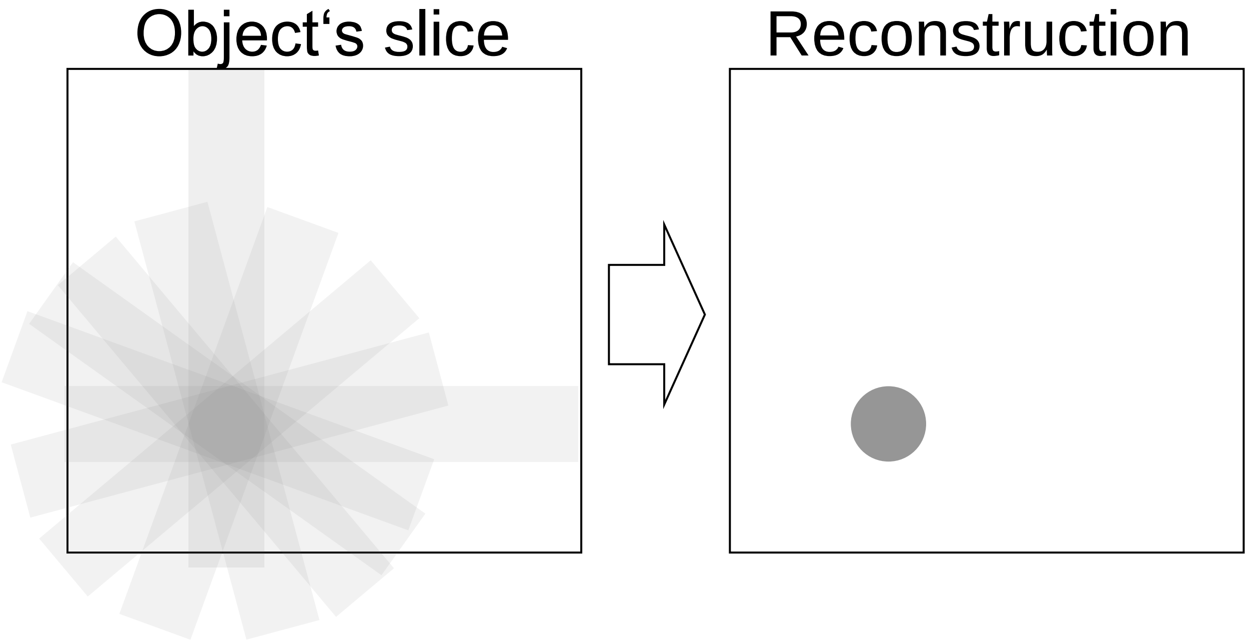

Tomography

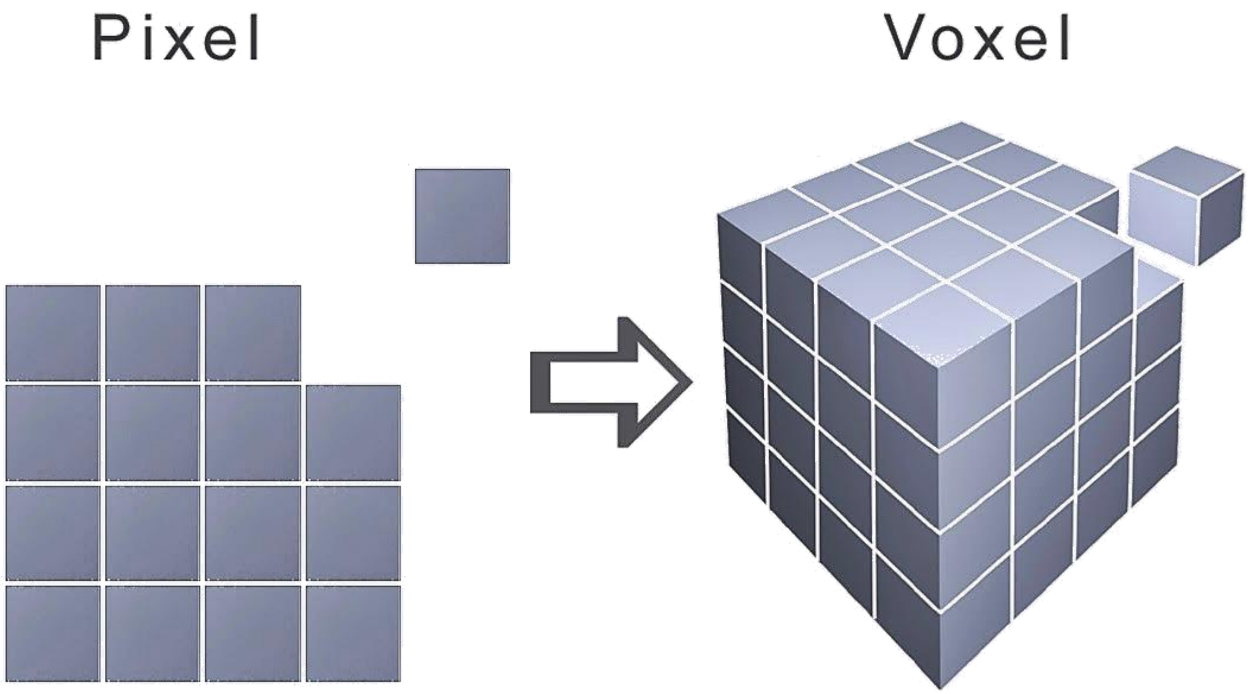

Radiography
(2D image of the transmission~$e^{-\Sigma d}$)

Tomography
(3D matrix of the attenuation coefficients Σ)

Tomography

Example: Lead ingots from shipwrecks

https://commons.wikimedia.org/wiki/File:Europe_180ad_roman_trade_map.png

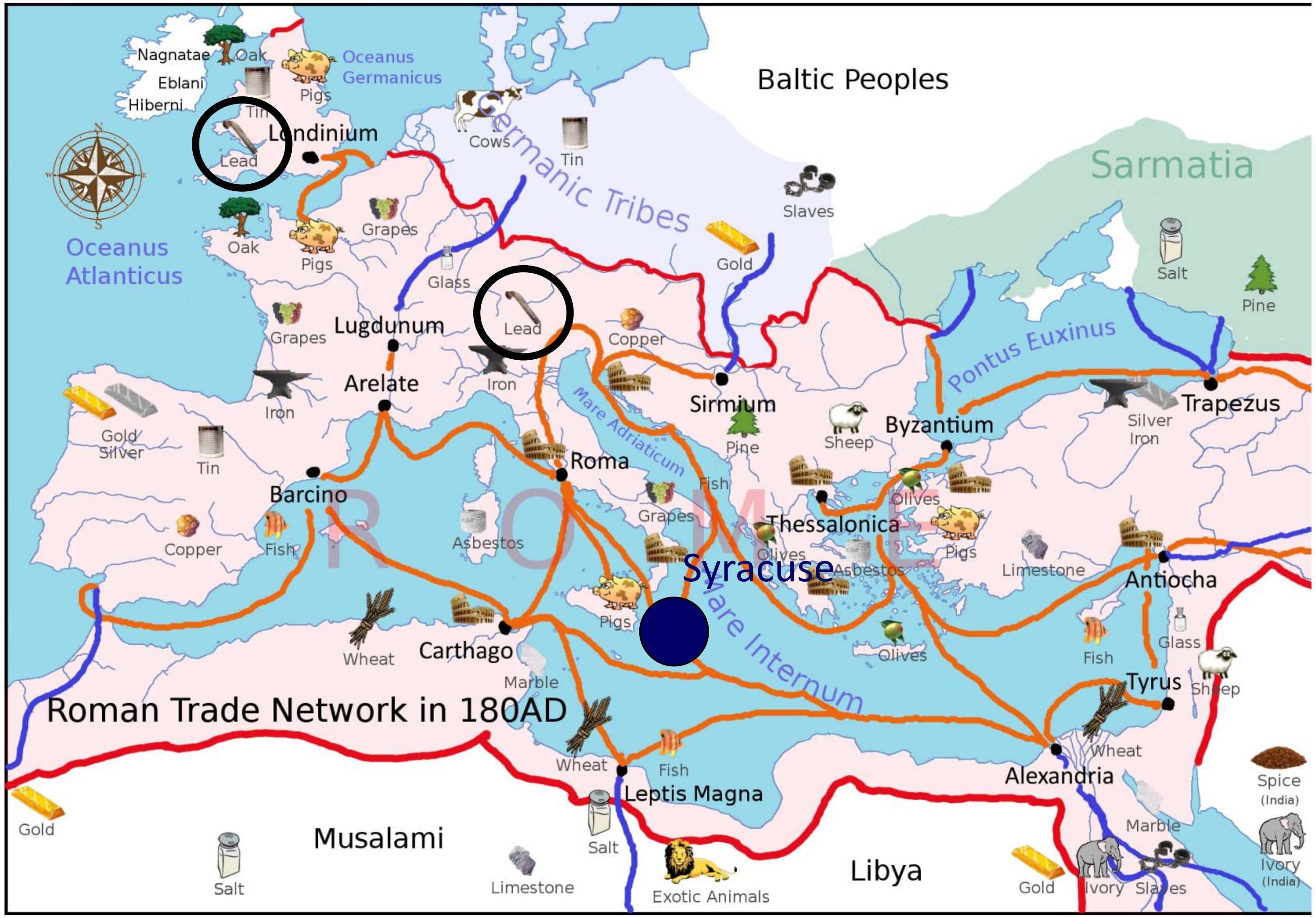

All routes lead to Rome: A map of Roman ports and trade routes

Tomography

Lead blocks recovered near the UNESCO World Heritage Site Syracuse. Presumably I century B.C. (Roman Imperial Age).

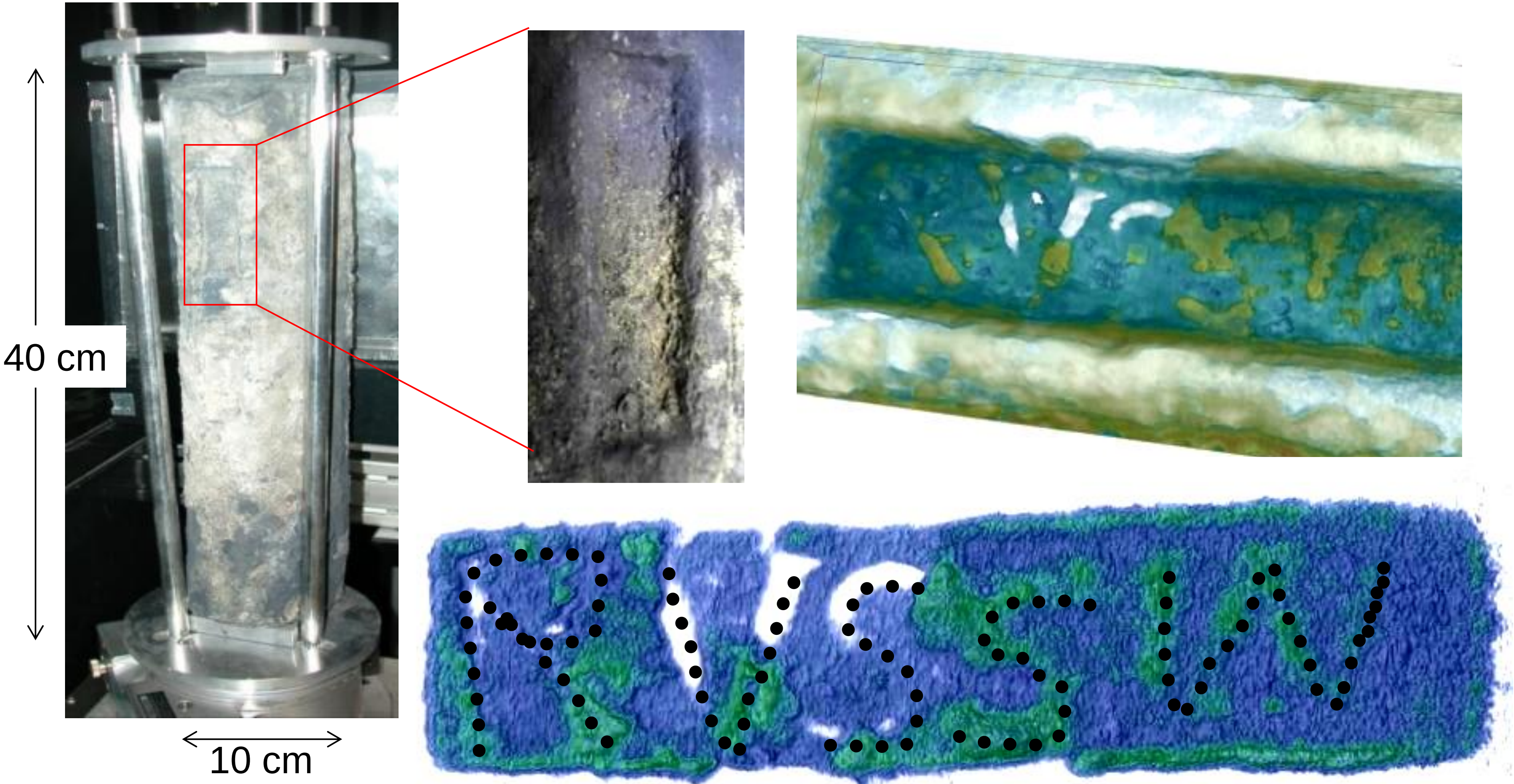

Triolo, R. et al, Neutron tomography of ancient lead artefacts, Anal. Methods 6 (2014) 2390-2394

HZB Helmholtz Zentrum Berlin

Tomography

Lead blocks recovered near the UNESCO World Heritage Site Syracuse. Presumably I century B.C. (Roman Imperial Age).

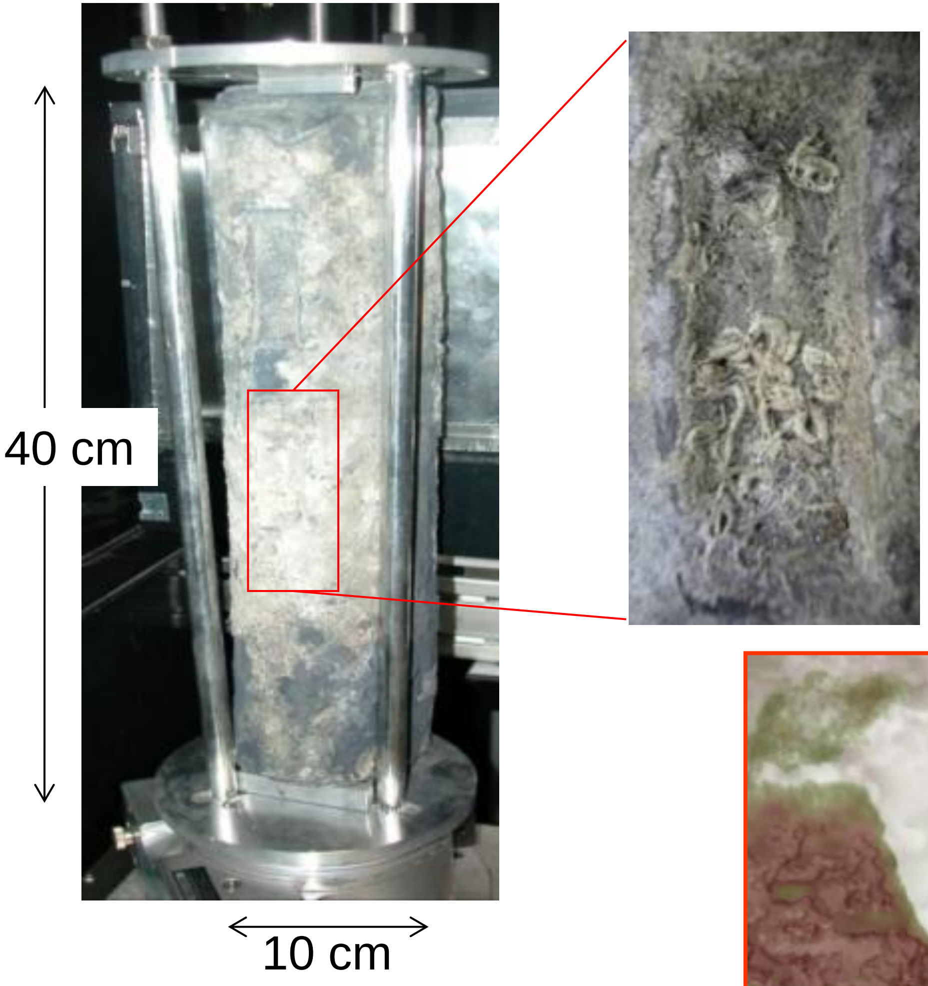

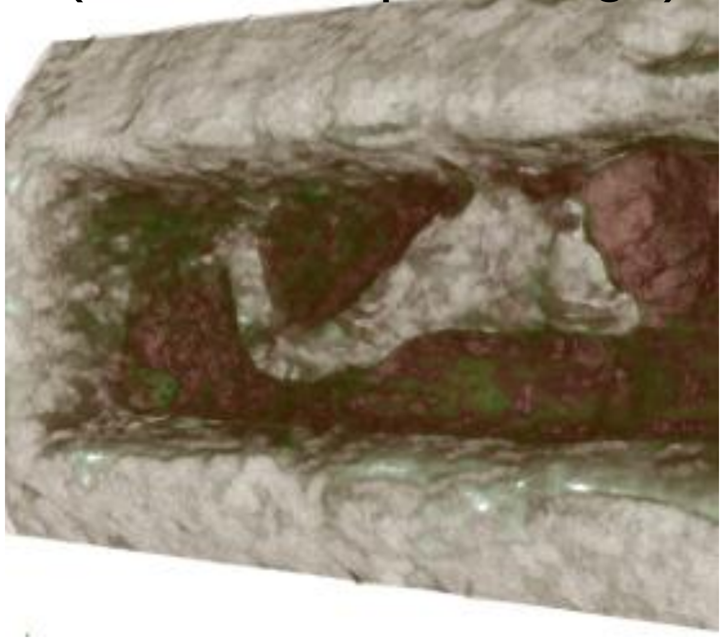

Tomography

Example: Lead ingots from shipwrecks

https://commons.wikimedia.org/wiki/File:Europe_180ad_roman_trade_map.png

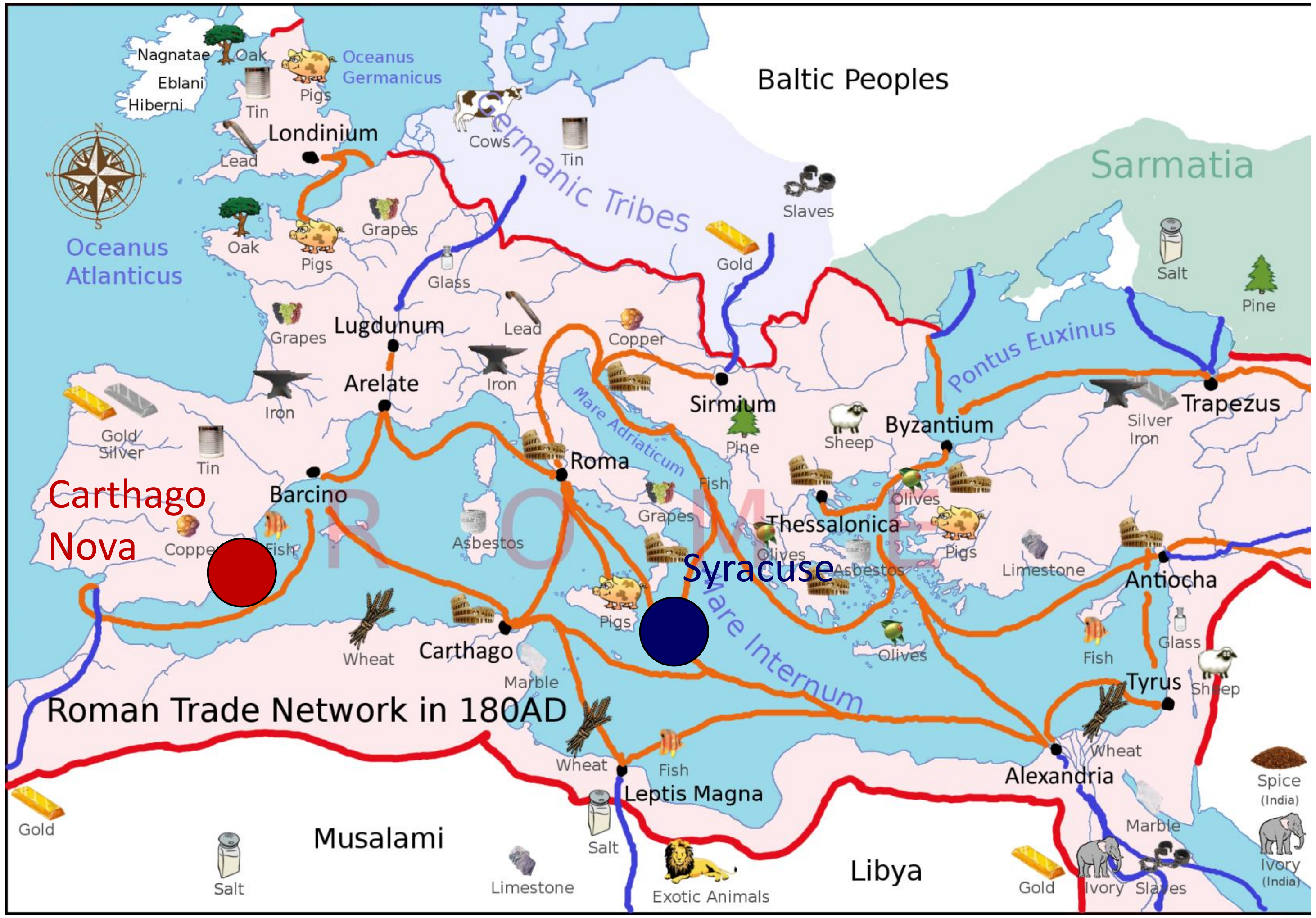

Triolo, R., et al. *Analytical Methods* 6.7 (2014): 2390-2394.

HZB Helmholtz Zentrum Berlin

Method development

High resolution

HZB concept

ILL design

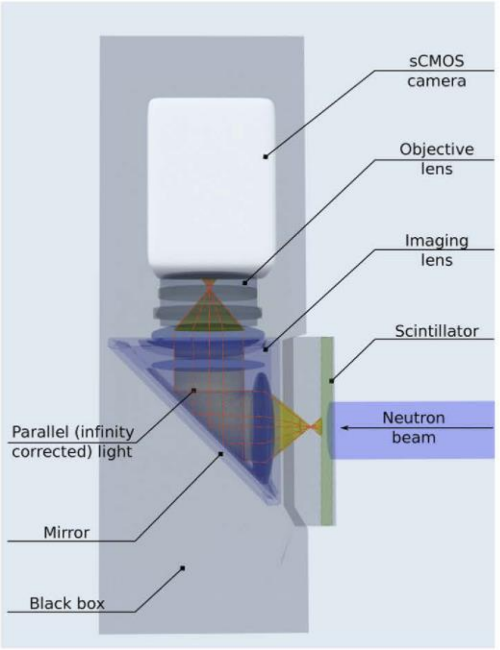

(a)

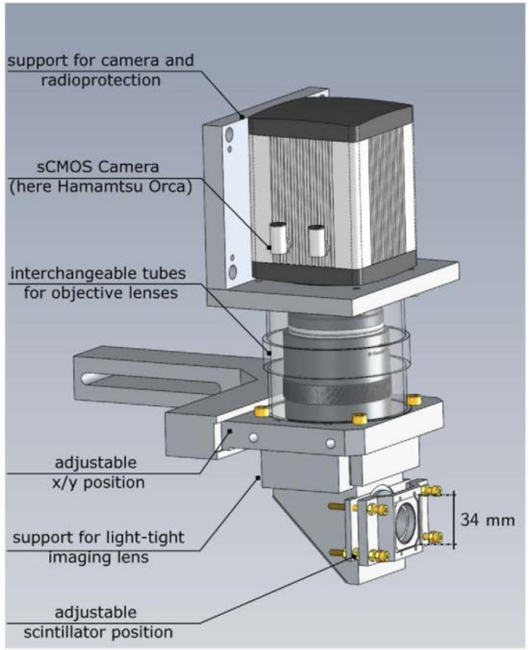

(b)

Resolution test
(GGG scintilator, pixel size 0.75 µm, exposure 13x1 min)

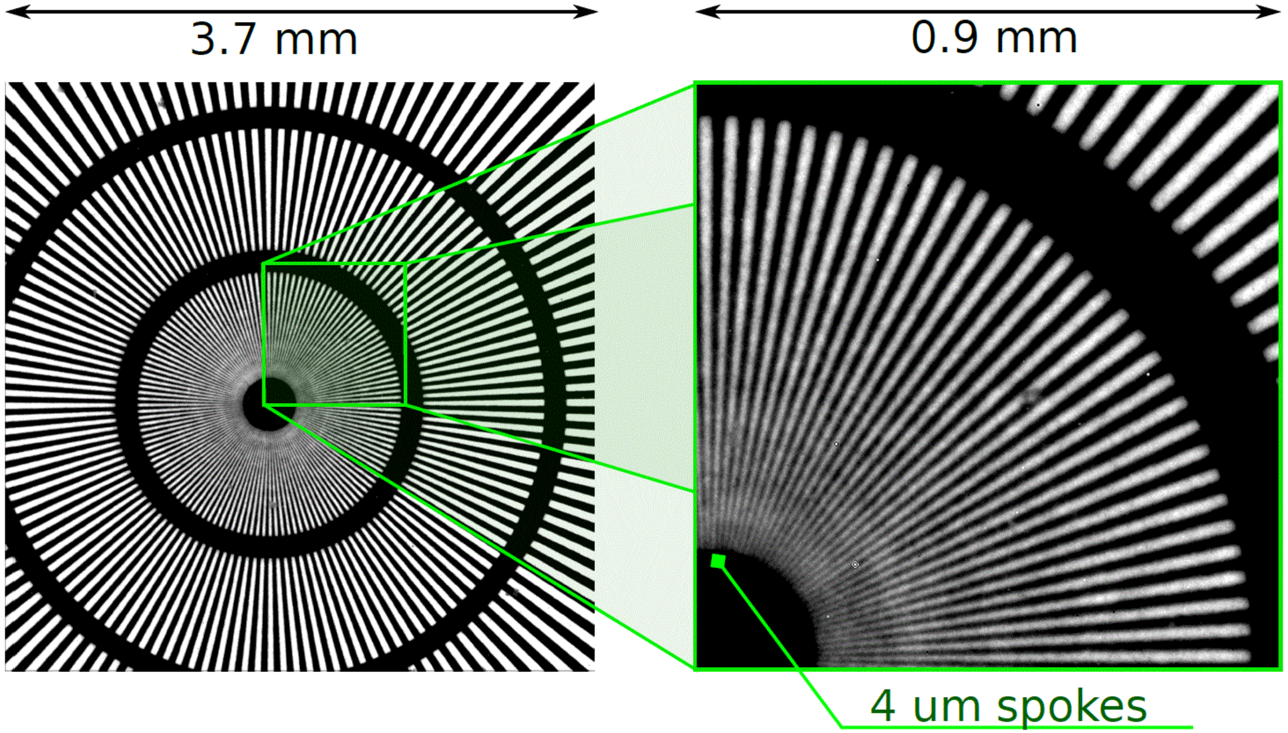

spatial resolution better than 4 µm

A. Tengattini et al. Optics Express 30.9 (2022)

Energy research: Dynamics of Li diffusion in batteries

4D Study of $SOCl_2$ Battery (pixel size: 8 µm, time step: 7.5 min)

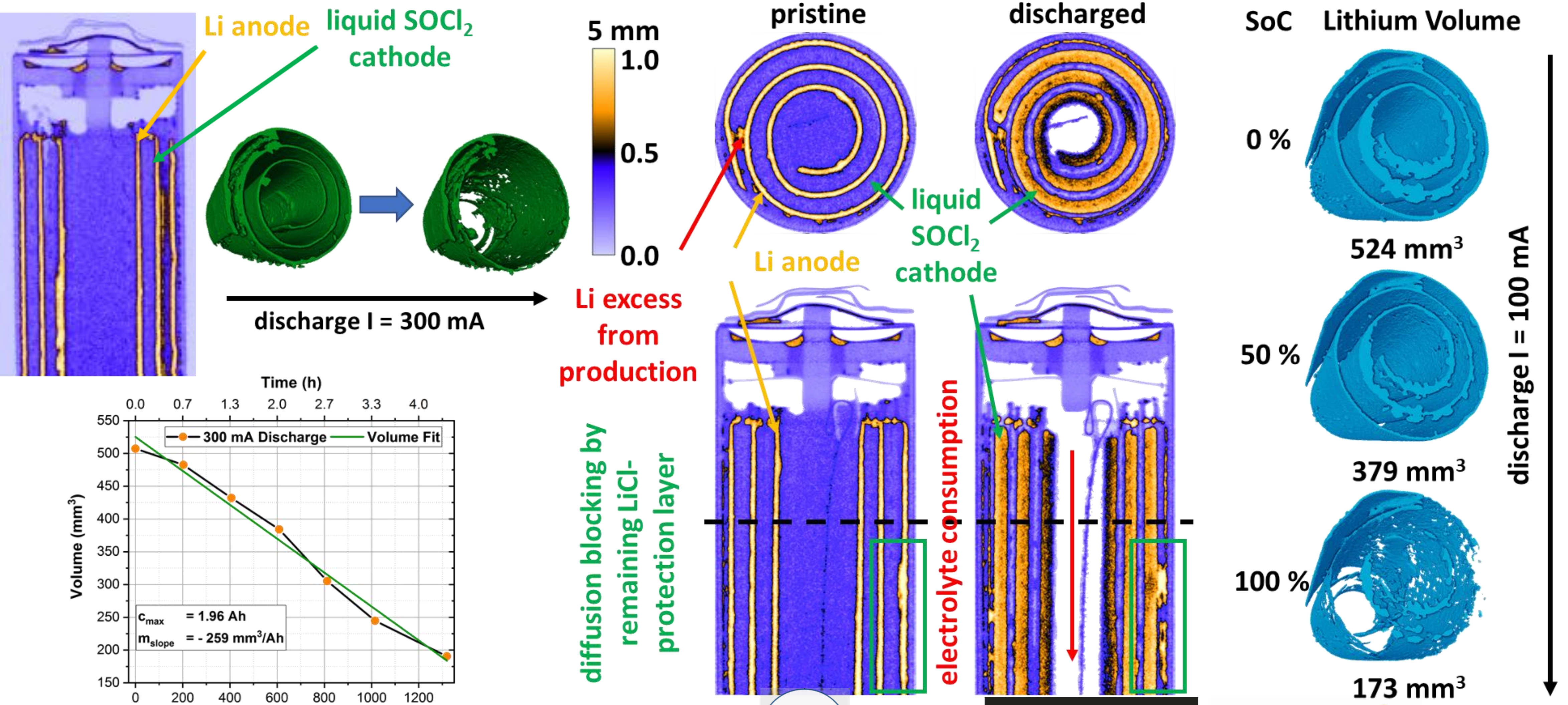

A. Tengattini
L. Helfen
Ralf Ziesche
Paul Shearing

R. Ziesche *et al*., Journal of Electrochemical Society 167 **(2020)**

Quantification of Li transport in batteries

Solid state battery

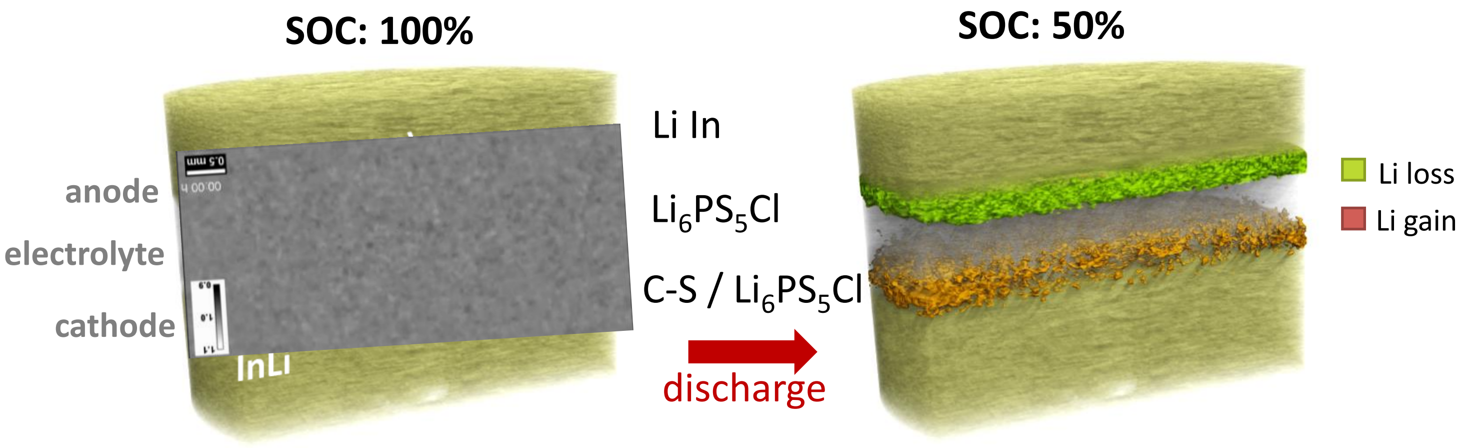

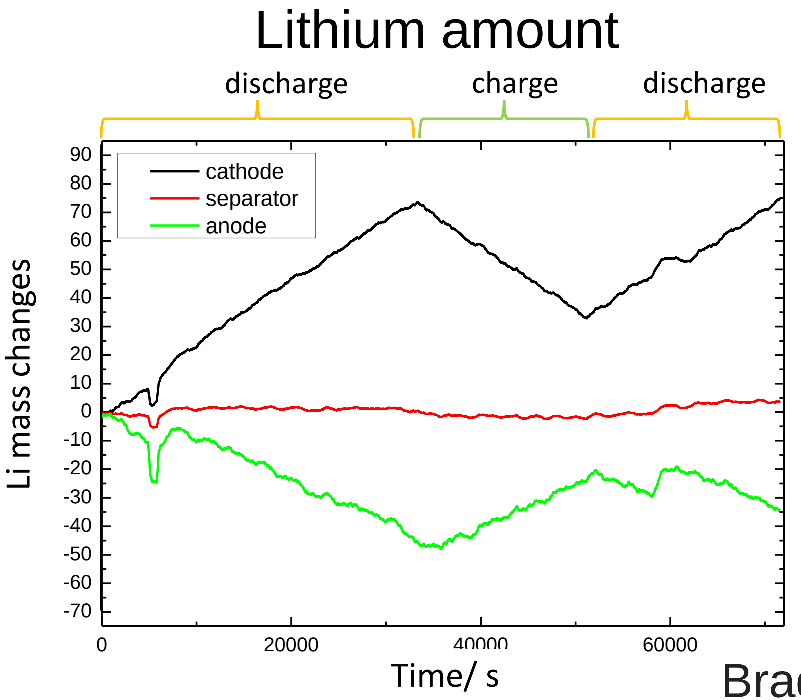

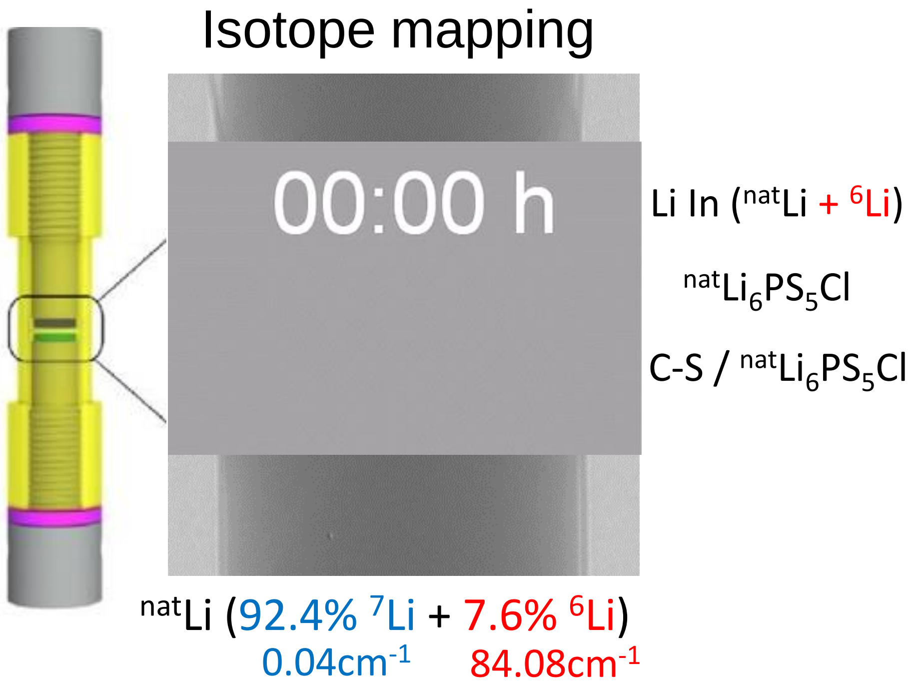

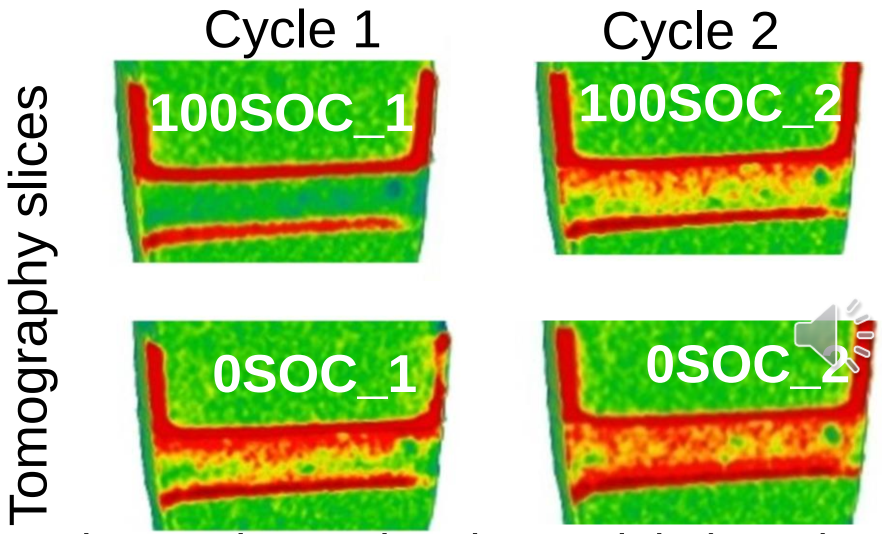

Bradbury, Robert, et al. *Advanced Functional Materials* (2023): 2302619.

Particle-wave duality

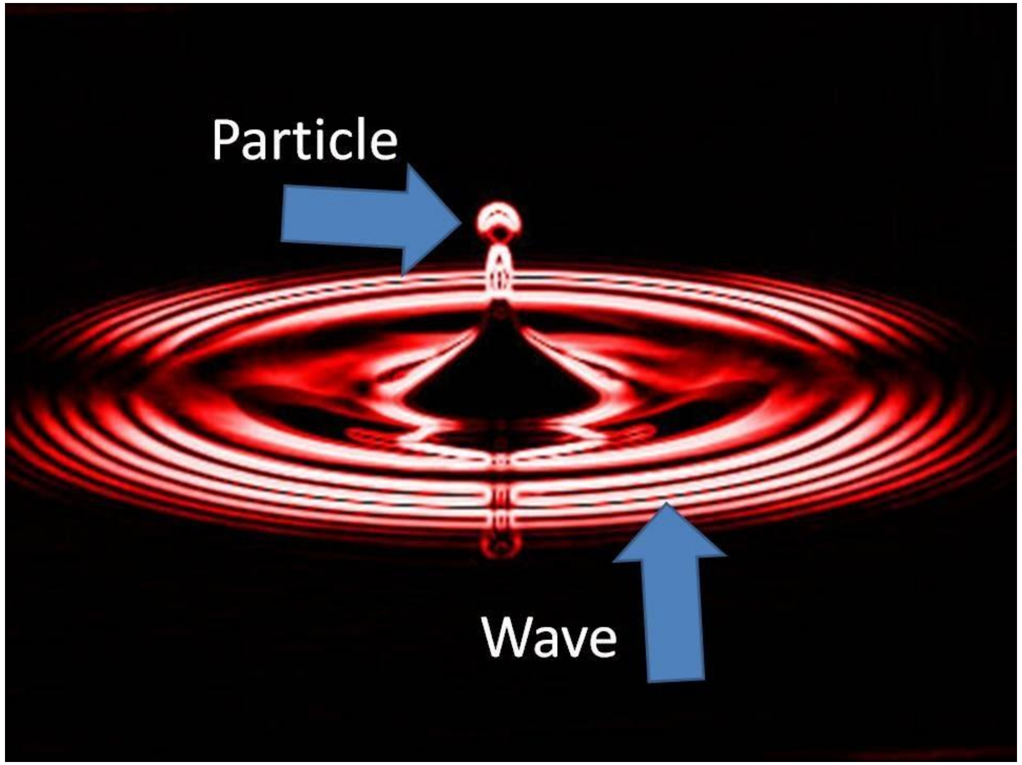

- de-Broglie wavelength: $\lambda = \frac{2\pi\hbar}{mv}$,
- Wave number: $k = 2\pi/\lambda$, $\mathbf{k} = \frac{m_n \mathbf{v}}{\hbar}$.
- Momentum: $p = \hbar k$
- Momentum operator: $\hat{\mathbf{p}} = -i\hbar\nabla$
- Kinetic energy: $E = \frac{\hbar^2 k^2}{2m_n}$,

Wave–particle duality is the concept in quantum mechanics that every particle may be partly described in terms not only of particles, but also of waves.

Hence the material particles like neutrons, also have wave properties such as wavelength and frequency.

Method development

Beam monochromatisation

Double crystal monochromator:
PCG crystals (mosaicity of 0.8°)

Range: 2.0 – 6.5 Å

Resolution ($\Delta\lambda/\lambda$): ~ 3%

Neutron flux: ~ 4×10^5 n/cm^{2}s
(at λ=3.0 Å)

Beam size: 5 x 20 cm^2

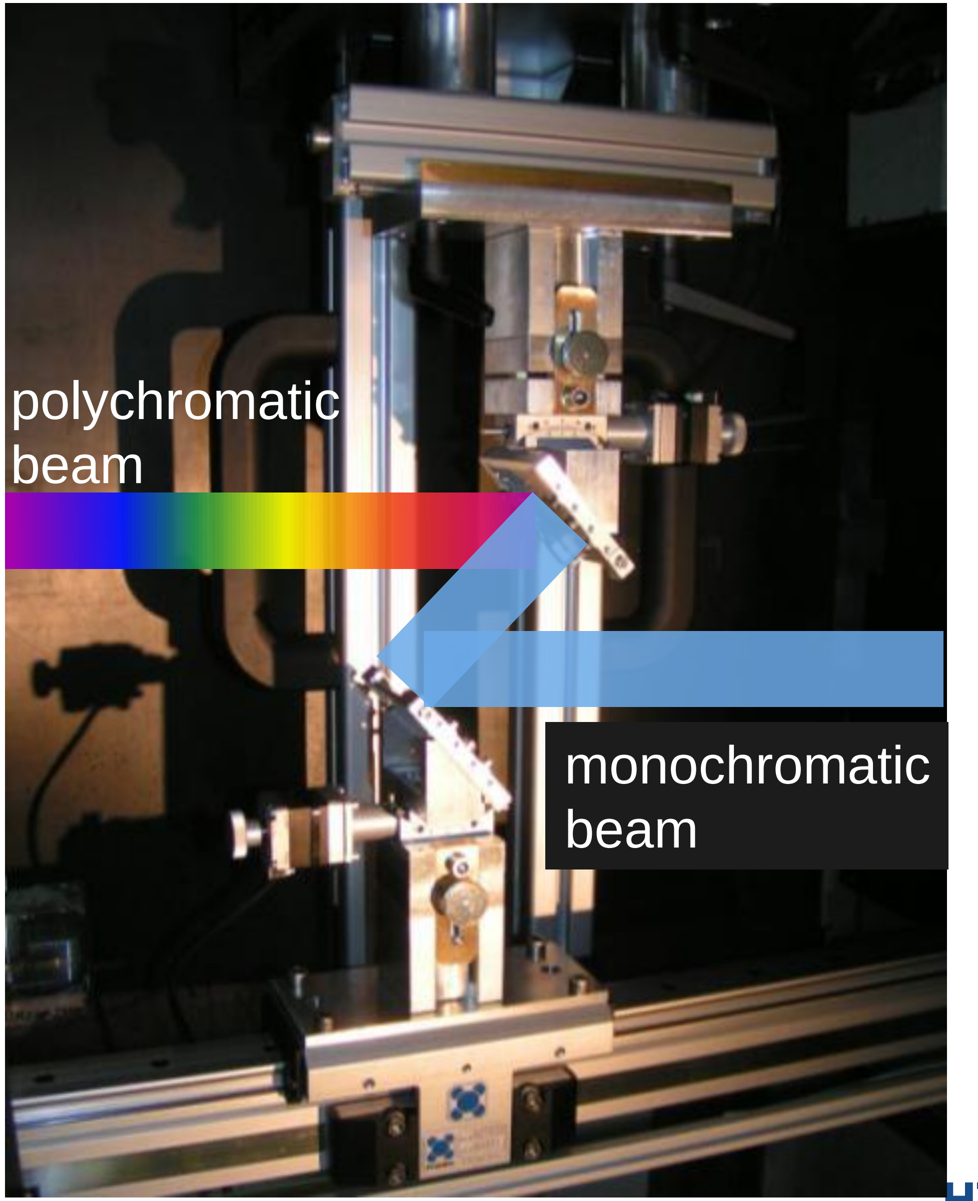

N. Kardjilov, et al. NIMA 605.1 (2009), 13-15.

Wavelength-selective imaging

Coherent scattering – Bragg edges

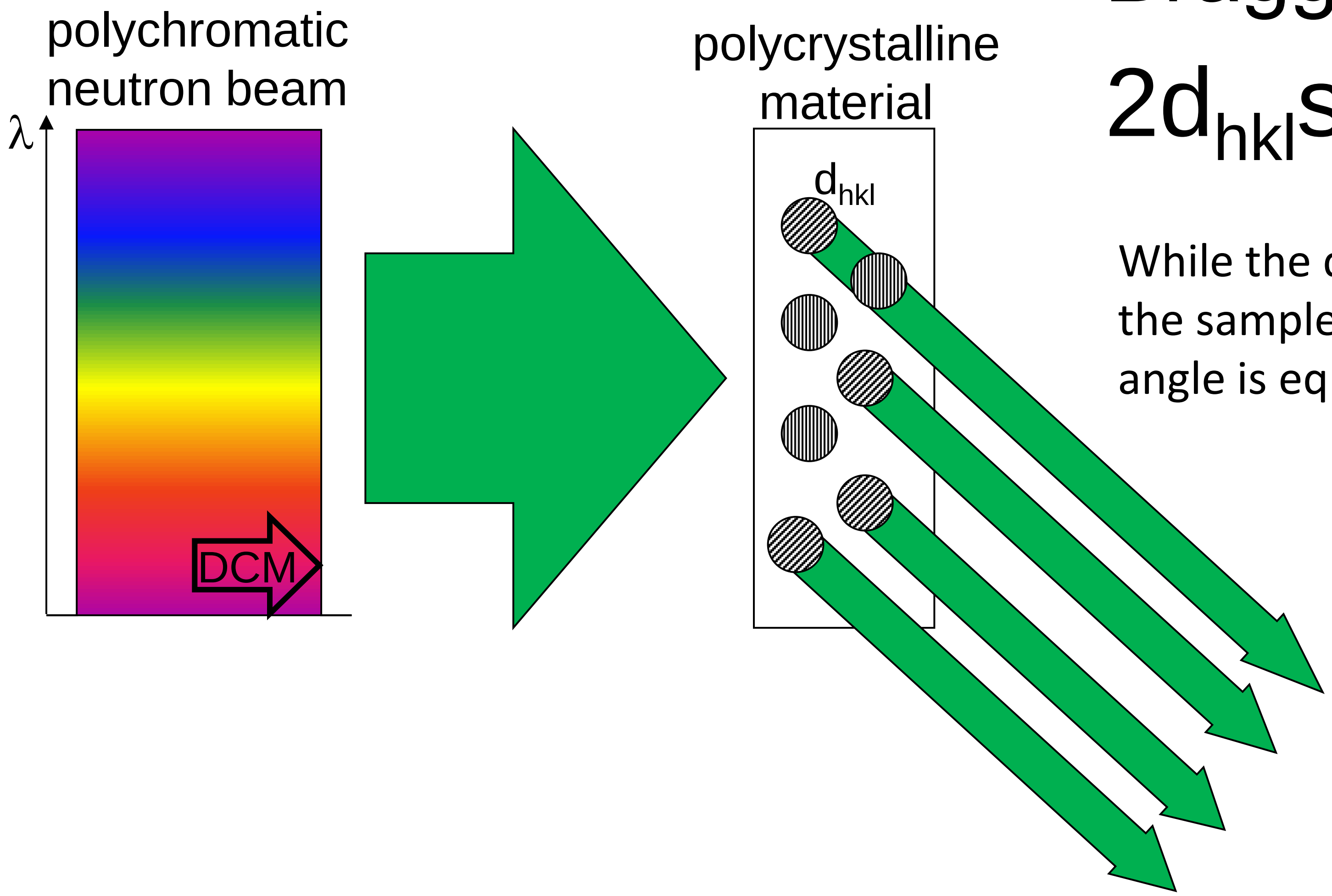

Bragg's law

$$2d_{hkl}\sin\theta=\lambda$$

While the detector is positioned behind the sample, the probed scattering angle is equivalent to 2θ=180˚.

For a given hkl family of lattice planes, the scattering angle increases as the wavelength is increased until the Bragg scattering condition can no longer be fulfilled by any orientation of a crystallite in the sample.

Wavelength-selective imaging

Coherent scattering – Bragg edges

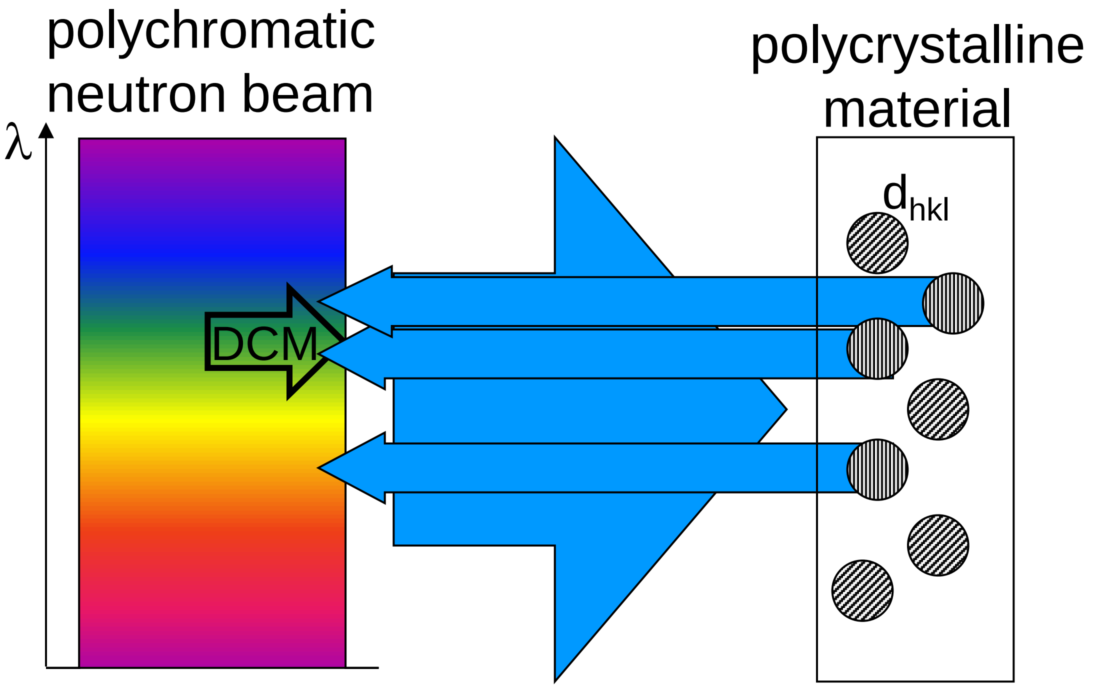

Bragg‘s law

$$2d_{hkl}\sin 90° = \lambda$$

Cross-sections of iron per atom

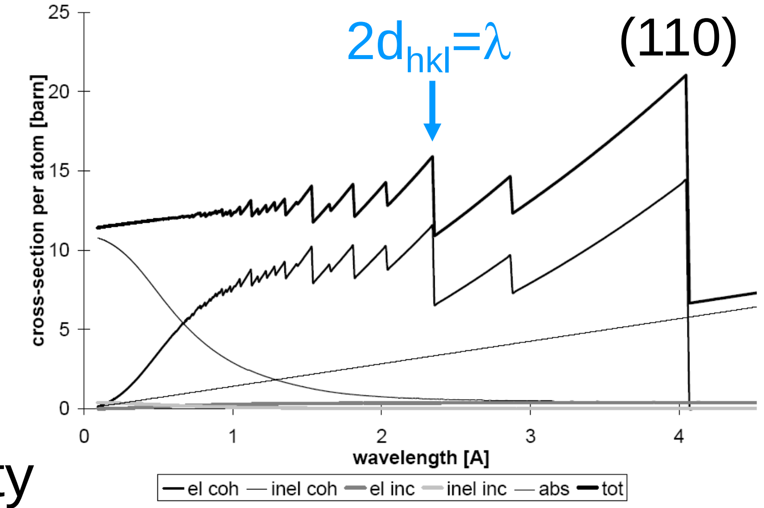

This occurs for wavelengths larger than
$\lambda = 2d_{hkl}\sin 90° = 2d_{hkl}$.
At this particular wavelength, the transmitted intensity increases markedly forming the so called Bragg edge.

Wavelength-selective imaging

Welded steel plates

Weld (photo)

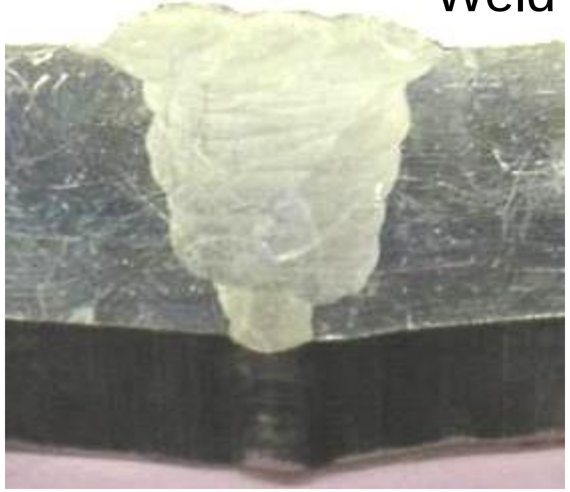

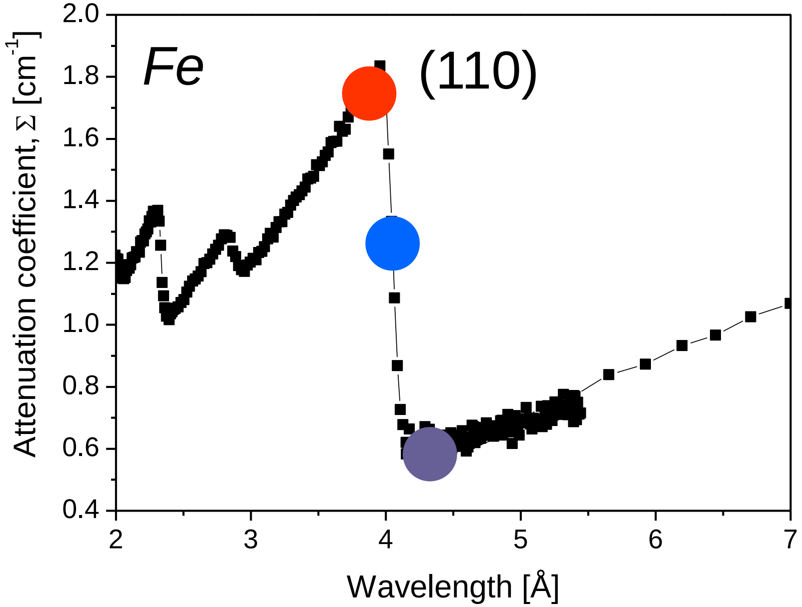

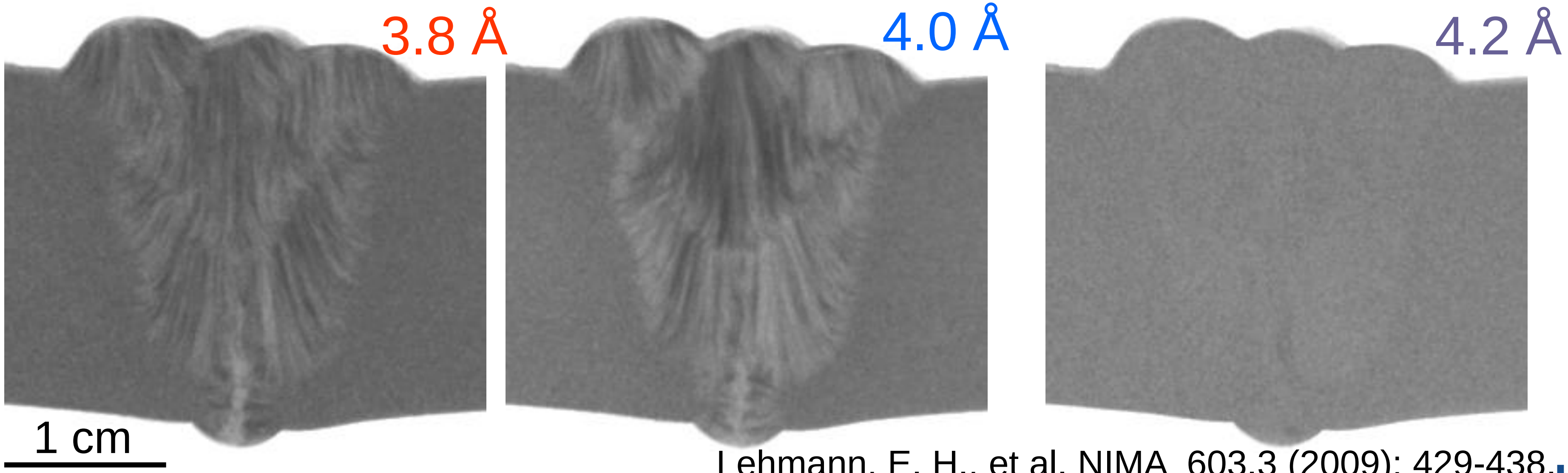

Lehmann, E. H., et al. NIMA 603.3 (2009): 429-438.

Wavelength-selective imaging

3D phase mapping in metals

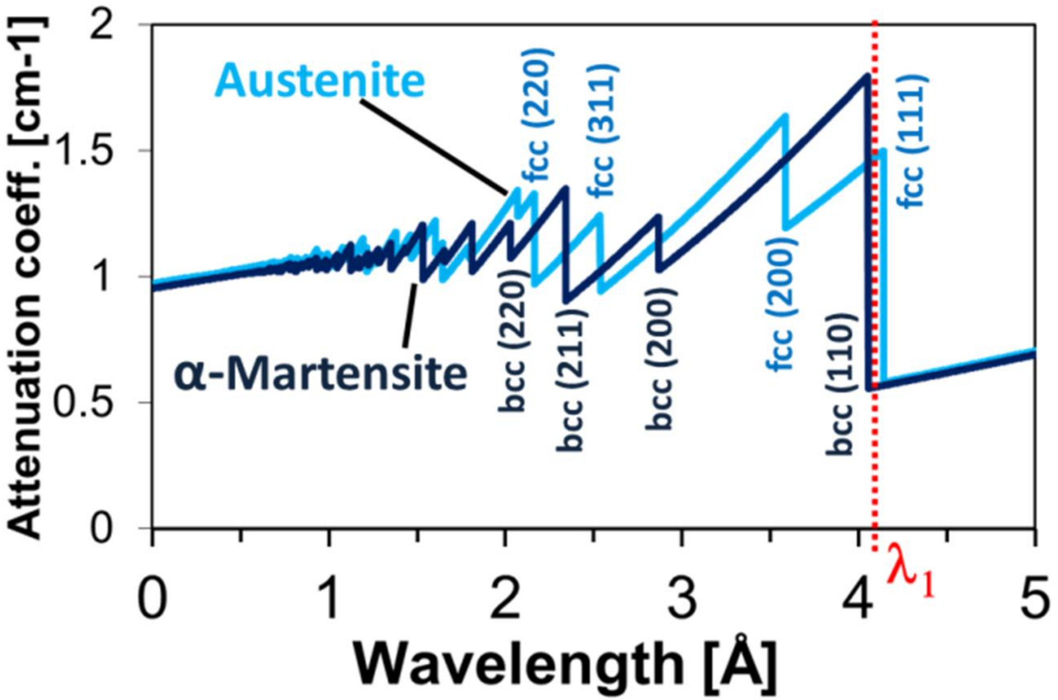

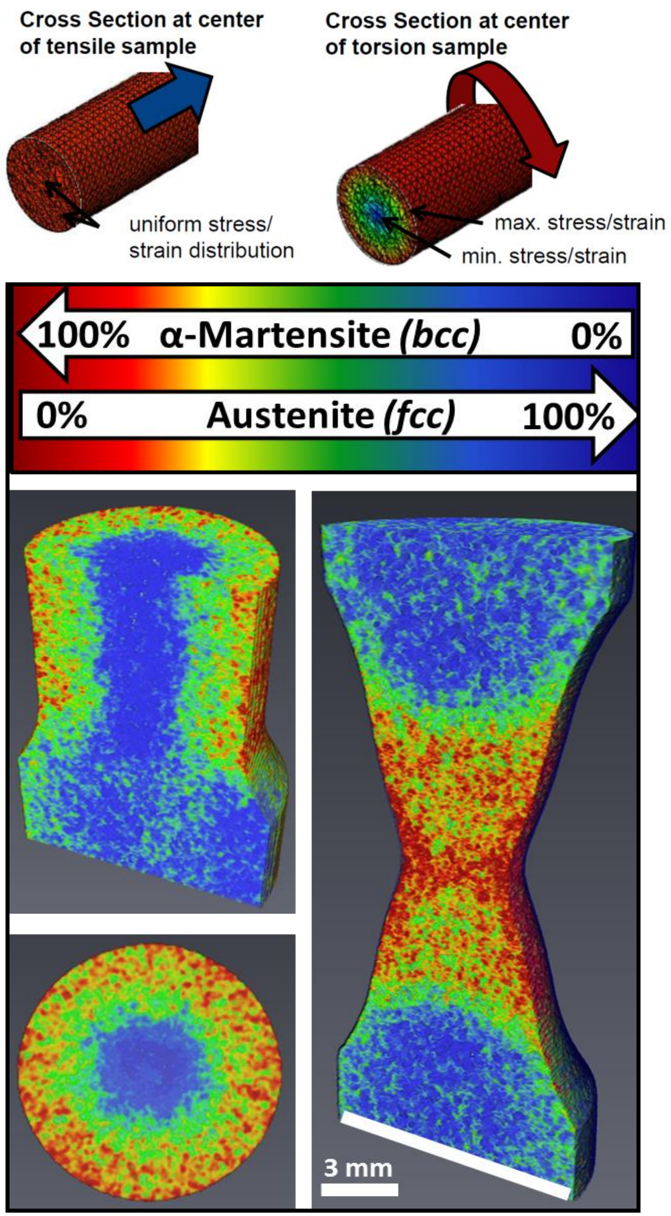

Energy-selective neutron tomography of TRIP-steel

R. Woracek et al., **Advanced Materials 26** (2014)

Wavelength-selective imaging

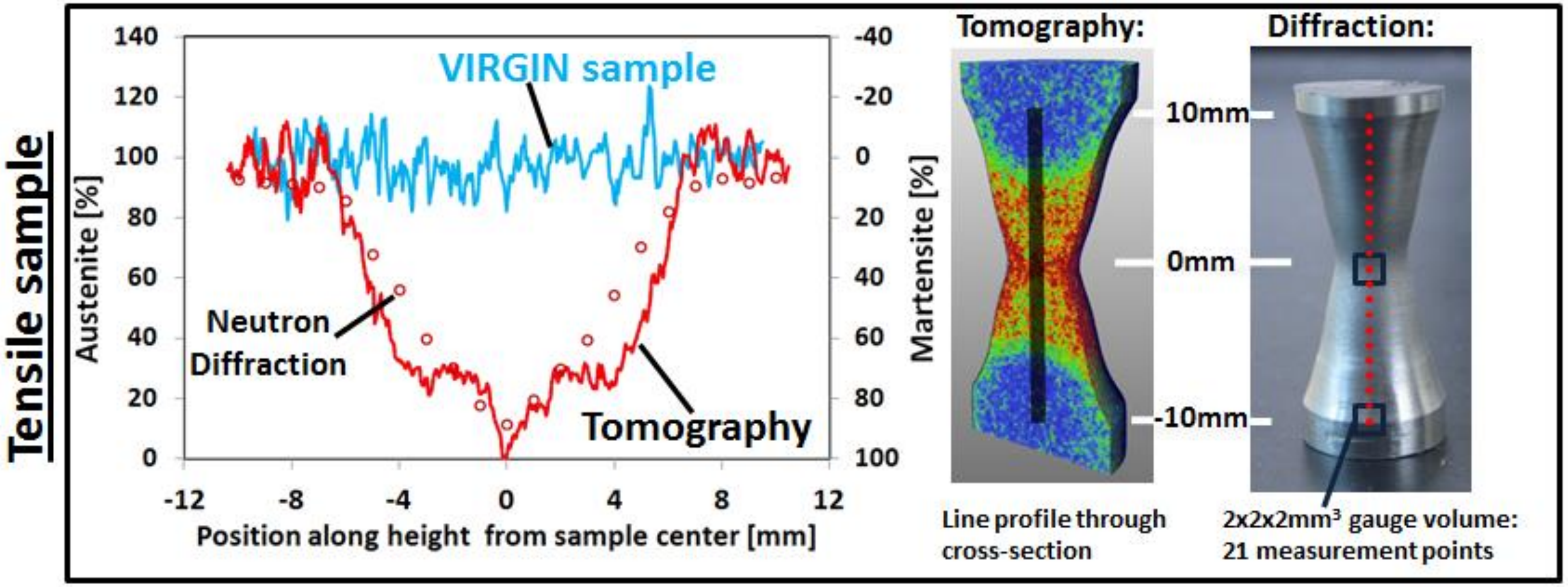

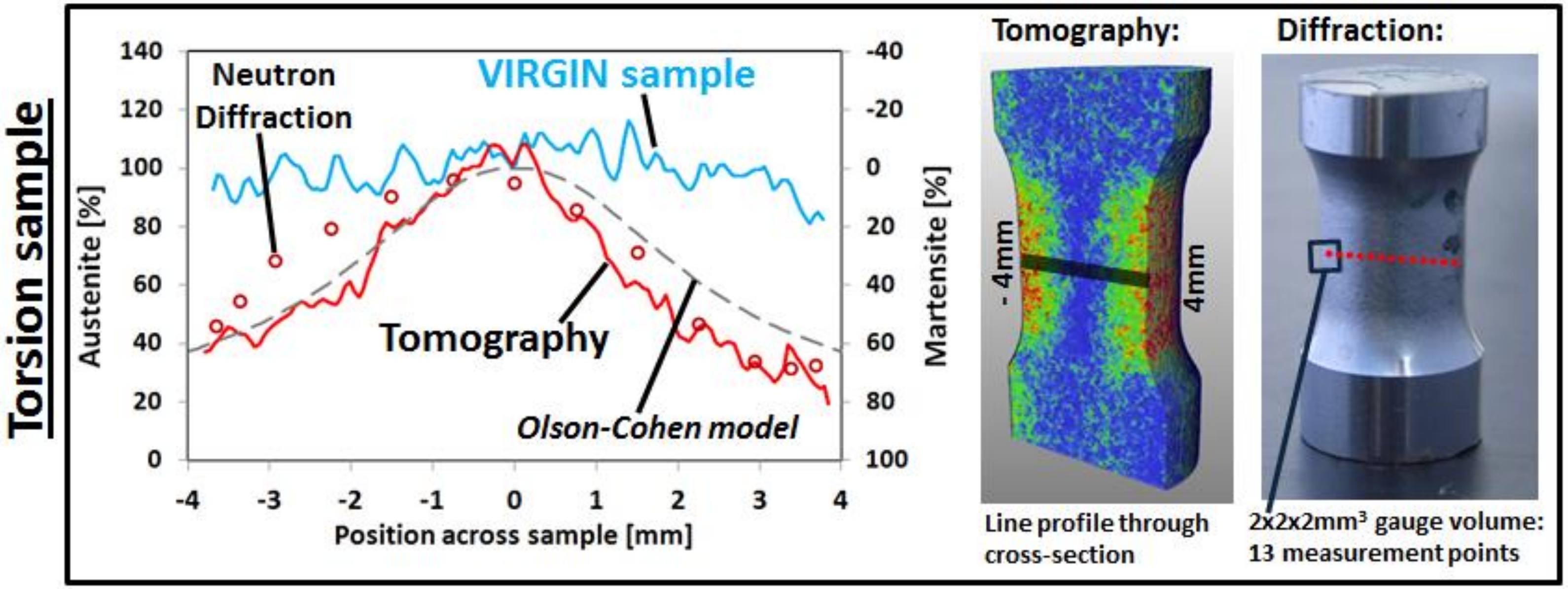

Imaging with polarized neutrons

Radiography image of a bar magnet taken with polarized neutrons

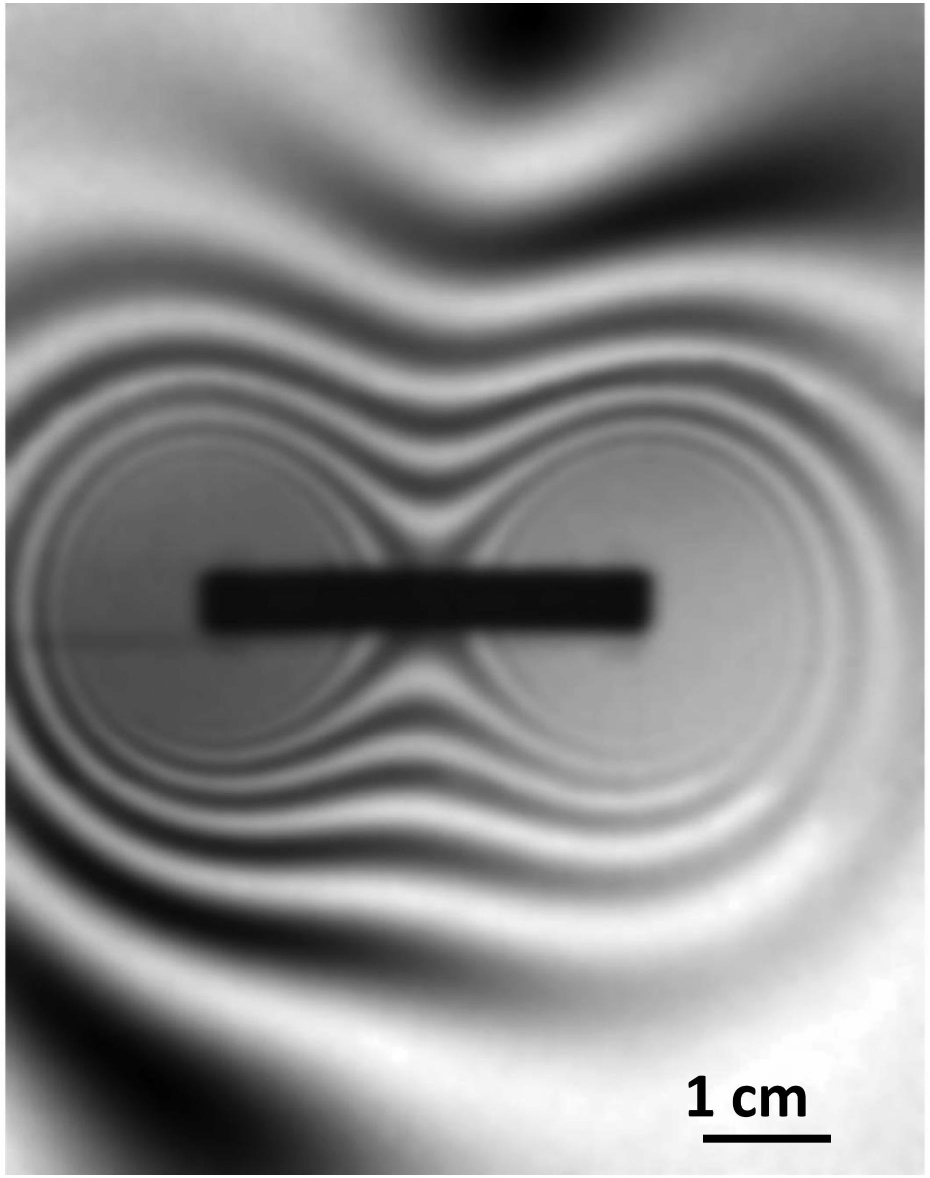

N. Kardjilov, et al,
Nature Physics 4, 399-403, (2008)

Imaging with polarized neutrons

Interactions of neutron spin with magnetic fields

Spin precession arround external magnetic field

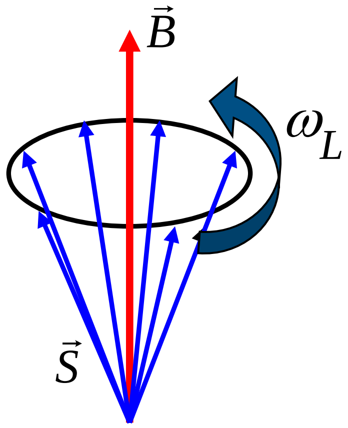

Larmor precession with a frequency:

$$\omega_L = \gamma B$$

$$\gamma = 1.83 \cdot 10^8 \frac{rad}{s \cdot T}$$ (gyromagnetic ratio)

The magnetic moment is antiparallel to the internal angular momentum of the neutron described by a spin S with the quantum number s = 1/2.

Kardjilov, Nikolay, et al. *Materials Today* 21.6 (2018): 652-672.

Imaging with polarized neutrons

Principle

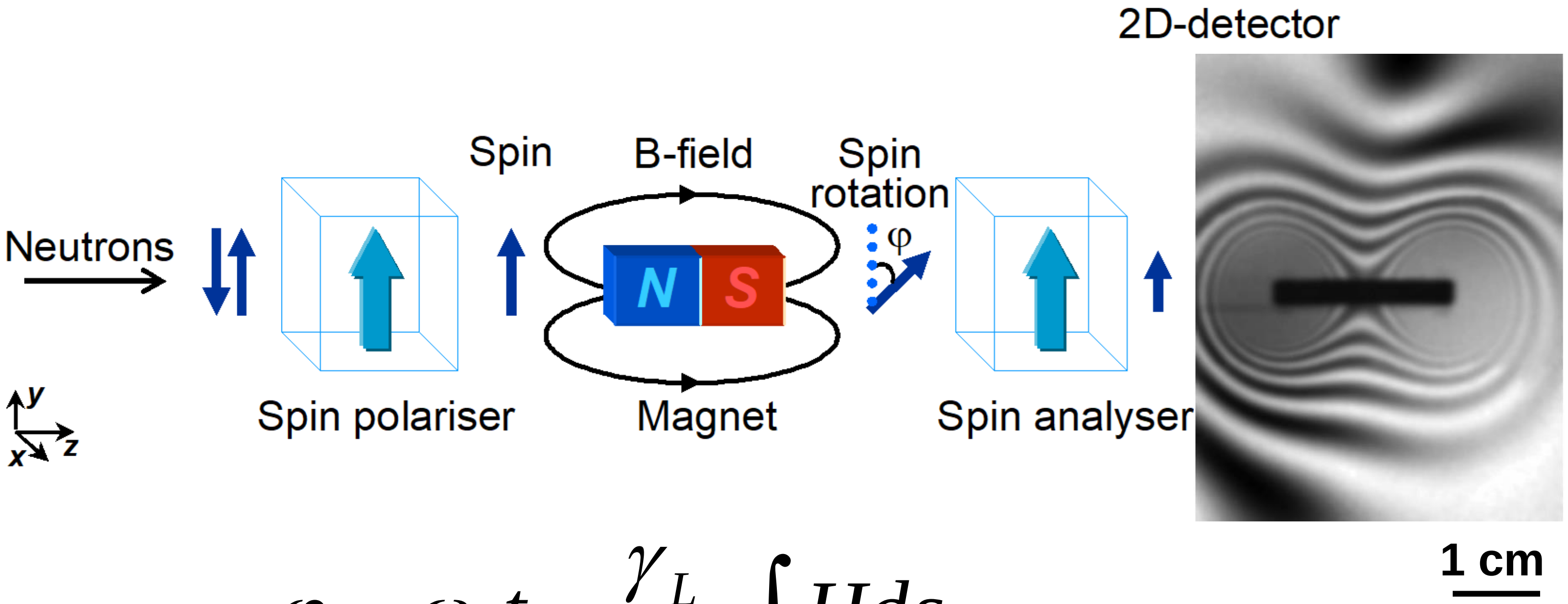

$$\varphi = \omega_L t = \frac{\gamma_L}{v} \int_{path} H ds$$

For the imaging setup, a polariser and analyser are used to select a defined neutron polarisation or orientation of the magnetic moment and to convert the precession angle φ of the neutron spin after transmission through the magnetic field or sample to imaging contrast, respectively.

N. Kardjilov, et al, Nature Physics 4, 399-403, (2008)

Imaging with polarized neutrons

Example: current coil

Radiography of magnetic field produced by a coper coil applying different currents using polarised neutrons

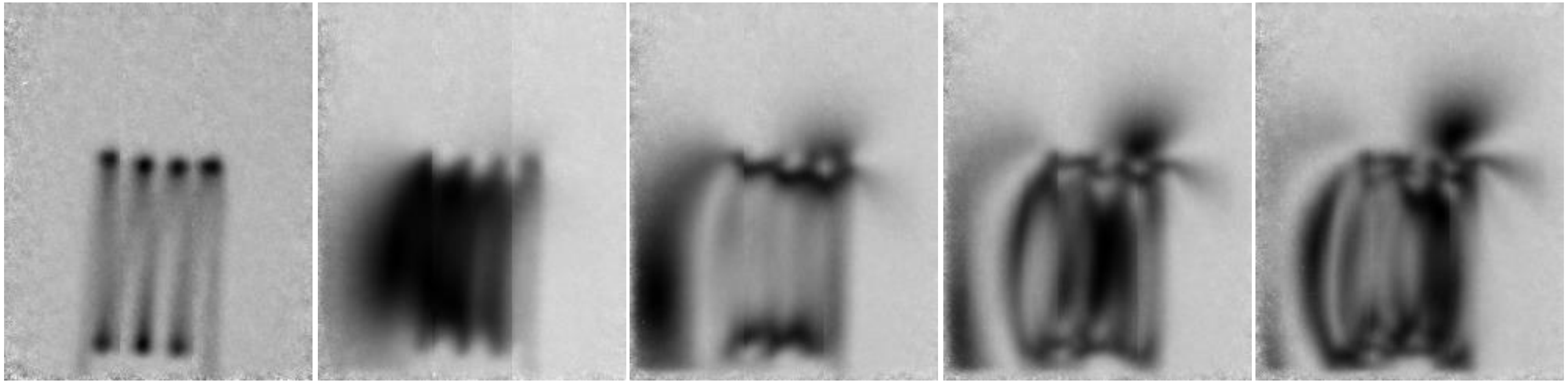

current: 0 Amp 4 Amp 8 Amp 12 Amp 15 Amp

For the imaging setup, a polariser and analyser are used to convert the precession angle φ of the neutron spin after transmission through the magnetic to imaging contrast, respectively.

Imaging with polarized neutrons

Example: permanent magnets

Polarised neutron radiography of magnetic field produced by permanent magnets

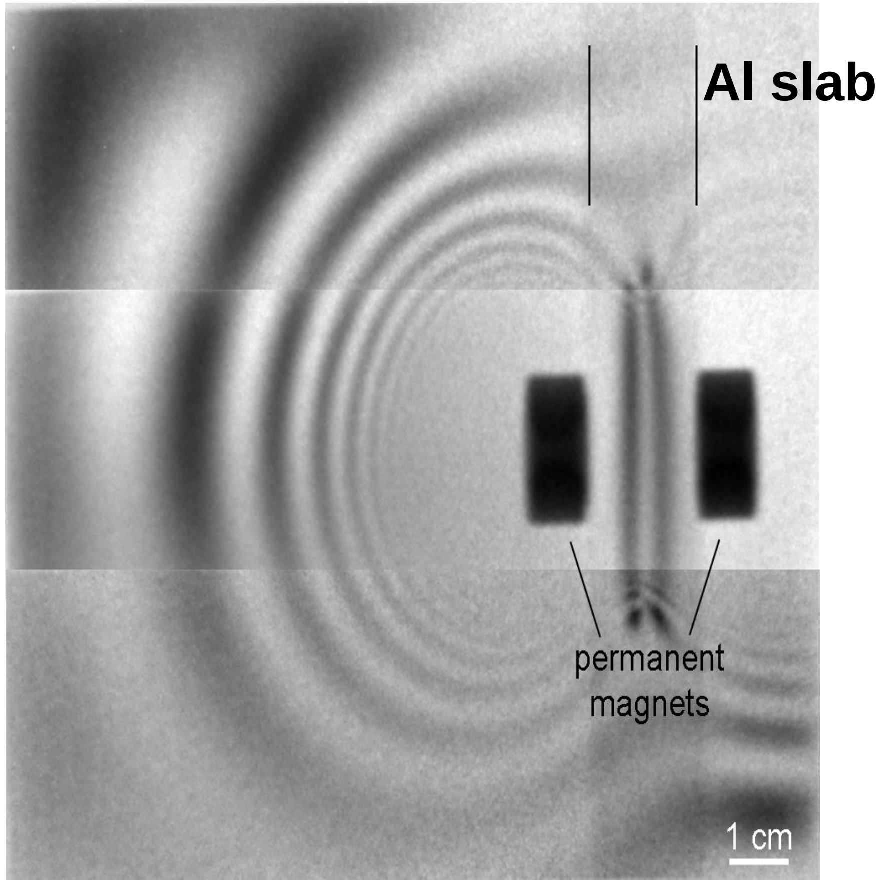

dipole magnets

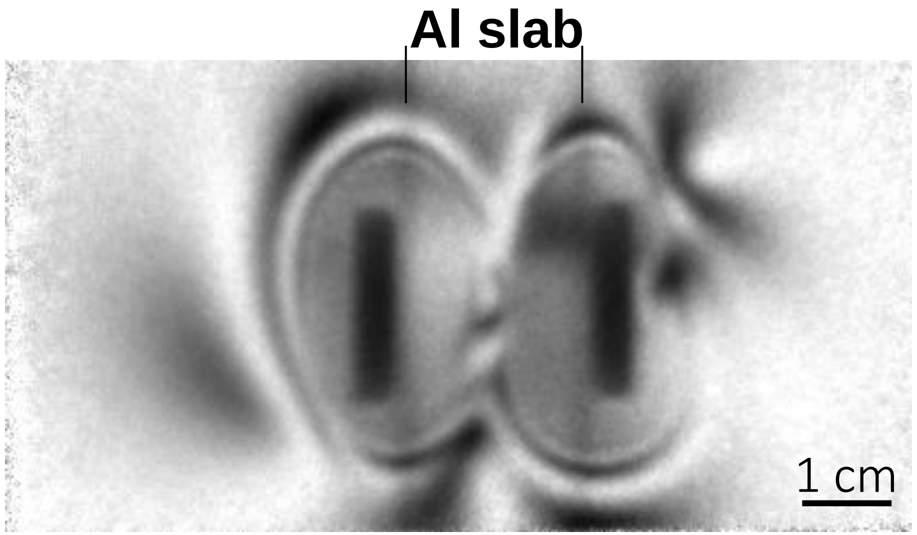

non-dipole magnets

Imaging with polarized neutrons

Simulations

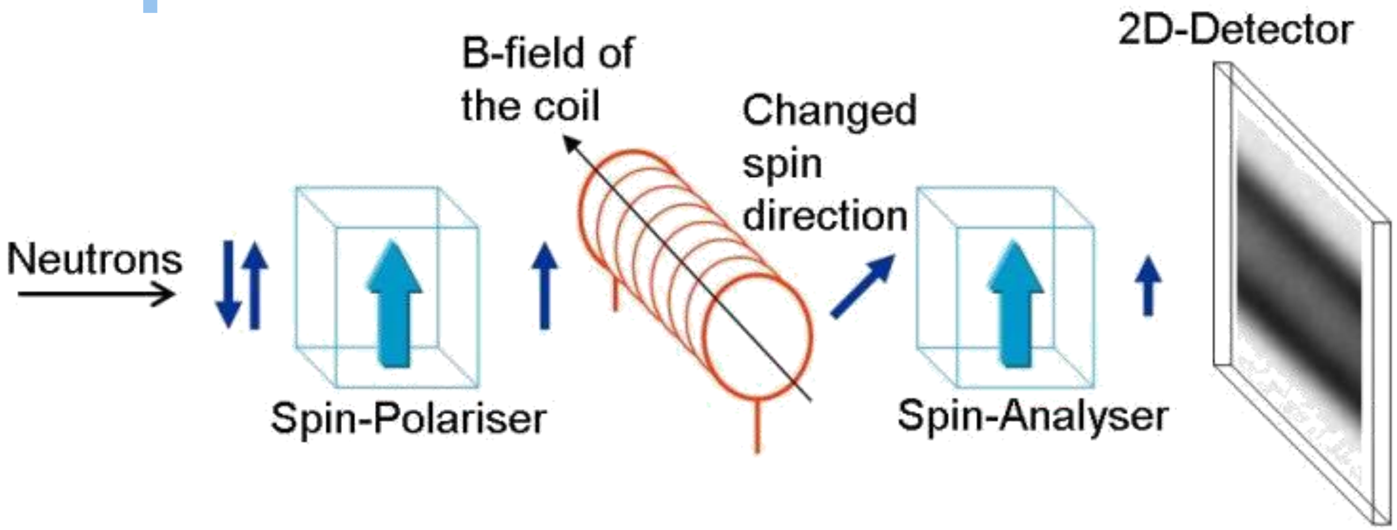

Biot-Savart law

$$d\vec{B} = \frac{\mu_0}{4\pi}\frac{Id\vec{l} \times \hat{r}}{r^3}$$

$$\phi = \frac{\gamma_L}{v}\int_{path} B ds$$

Spin rotation

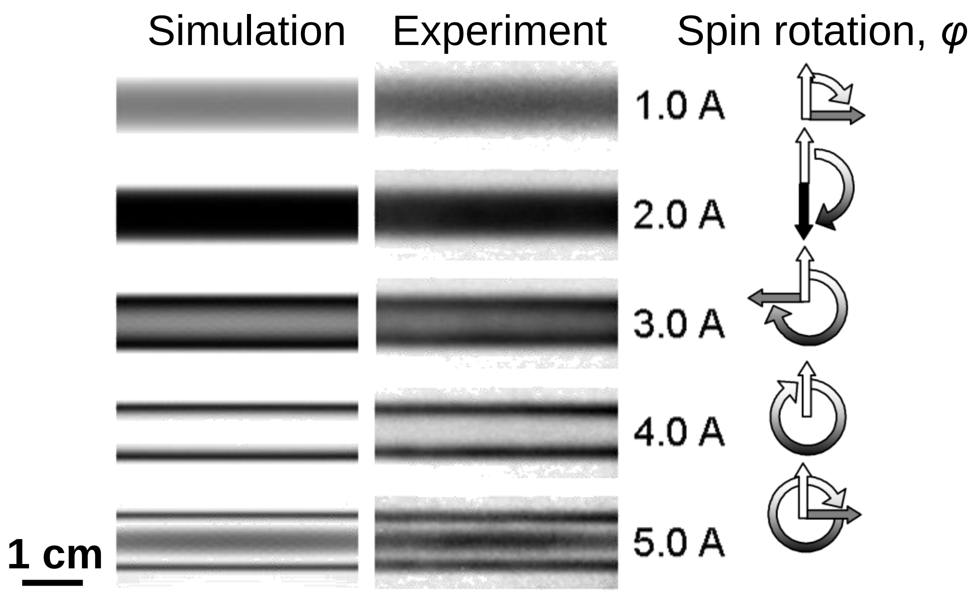

Imaging with polarized neutrons

High temperature superconductor

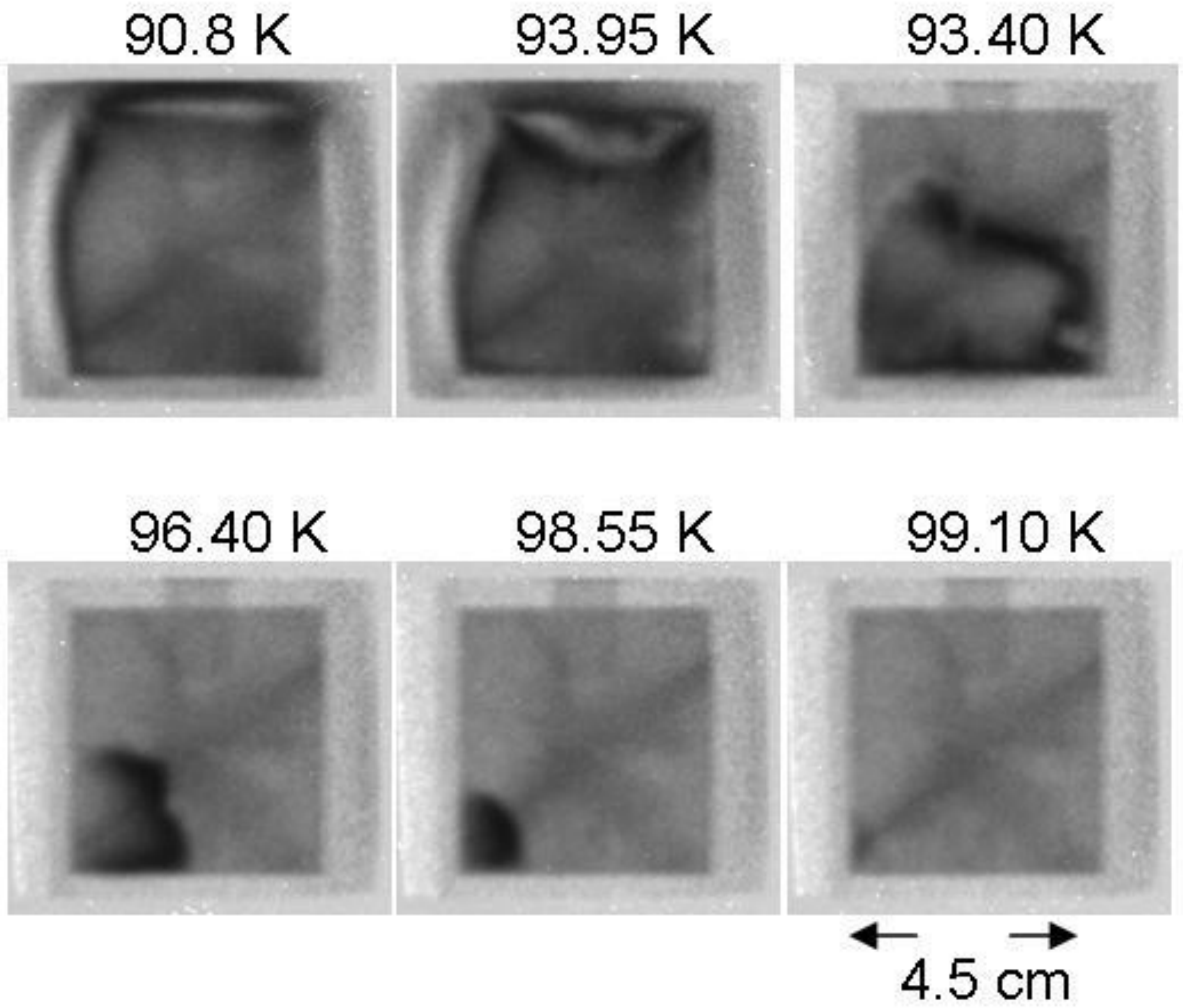

Flux trapping in a 45x45x12 mm^2 bulk YBCO sample.

Imaging with polarized neutrons

High temperature superconductor

Pb cylinder
(polycrystalline)

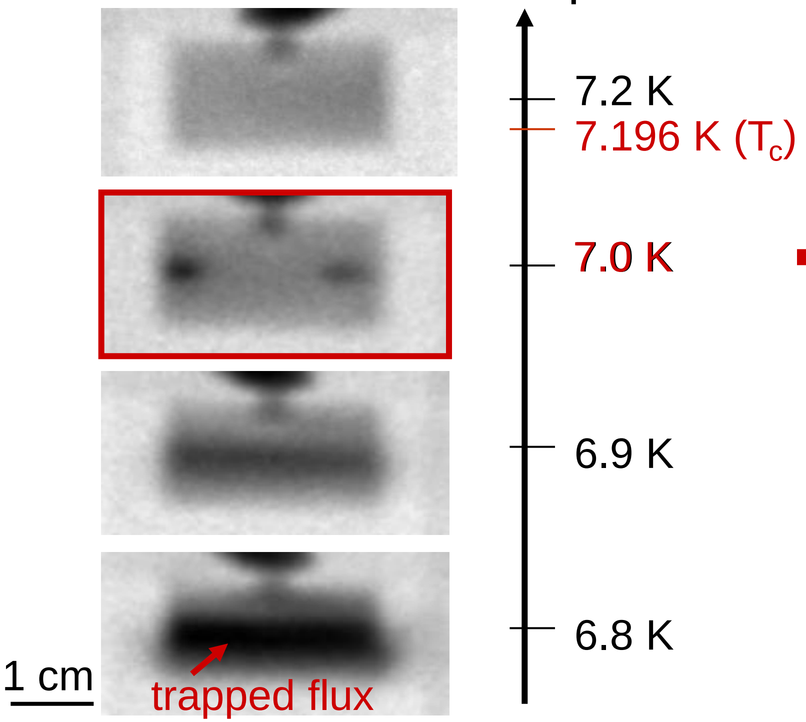

Tomography

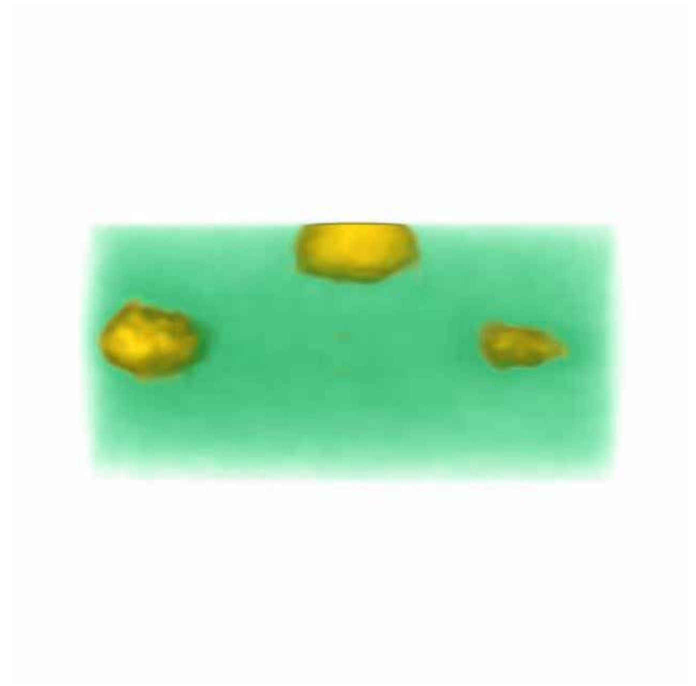

Flux pinning at cooling down below Tc while applying a homogenous magnetic field of 10 mT perpendicular to the beam.

The images were recorded after switching off the magnetic field.

Imaging with polarized neutrons

Tensorial tomography

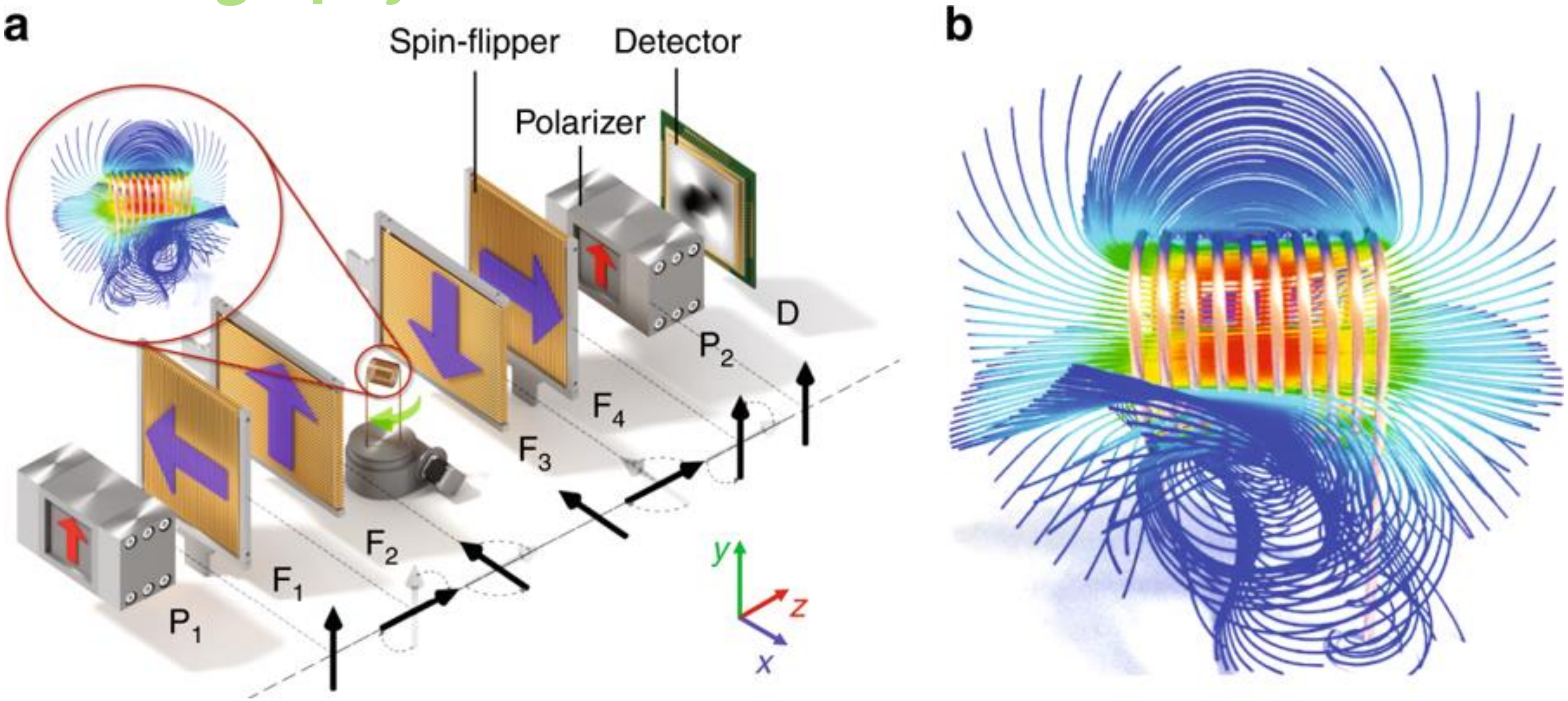

Tensor tomography. a Schematic drawing of the setup used for tensor tomography with spin-polarized neutrons, comprising spin polarizers (P), spin flippers (F) and a detector (D). b Selected magnetic field lines around an electric coil (calculation)

A. Hilger, et al, Nature Communications 9.1 (2018): 4023

Imaging with polarized neutrons

Tensorial tomography

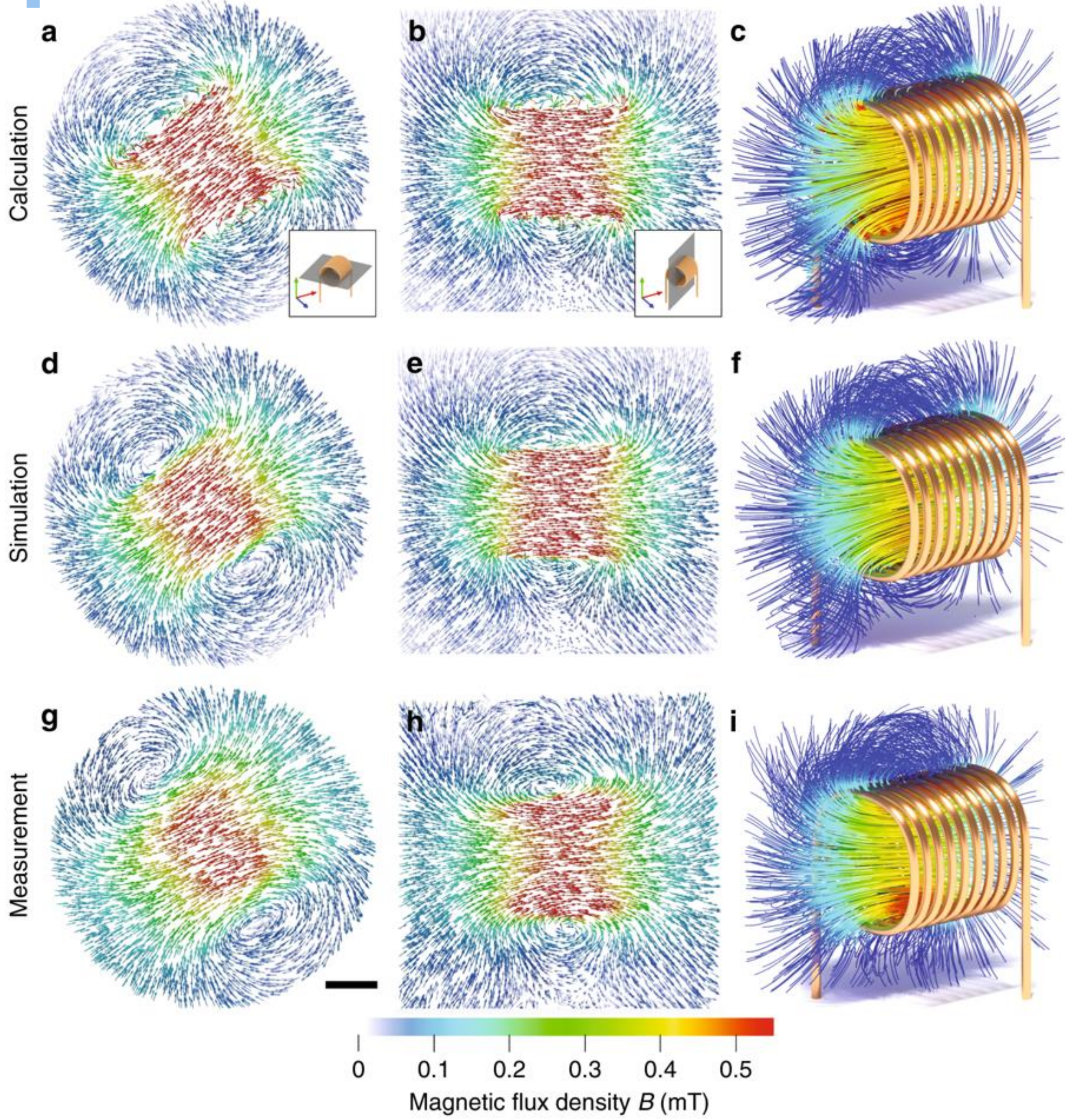

Imaging with polarized neutrons

Tensorial tomography

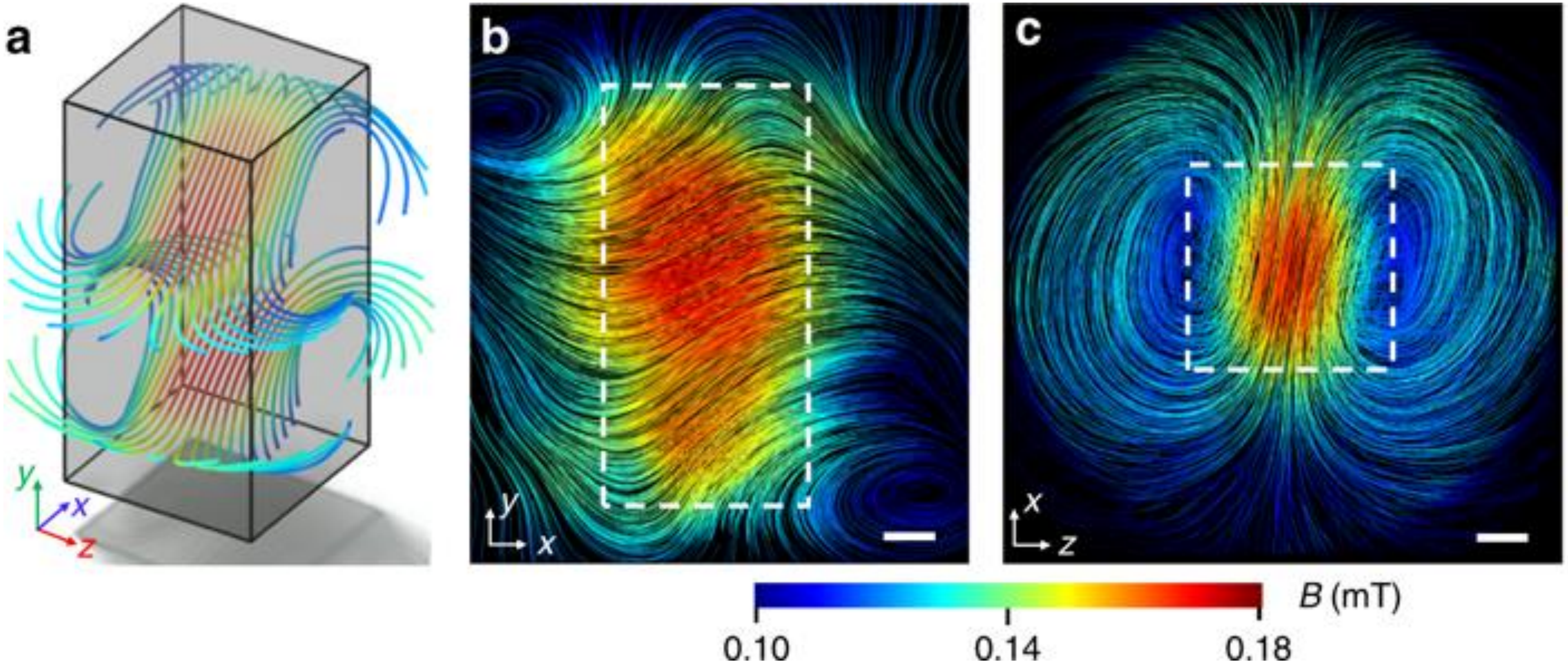

Magnetic vector field inside a superconducting lead sample measured at $T = 4.3$ K. a Some selected magnetic field lines show the location of the magnetic field inside the sample indicated by the cuboid. b Magnetic field lines in a selected *xy* plane (silhouette of the lead sample marked by dotted lines). Scale bar, 5 mm. c Magnetic field lines in a selected *xz* plane. Scale bar, 5 mm.

A. Hilger, et al, Nature Communications 9.1 (2018): 4023

Conclusion

Why Neutron Imaging?

- High sensitivity to Li and H (Contrast)
- Different attenuation coefficient for Isotopes

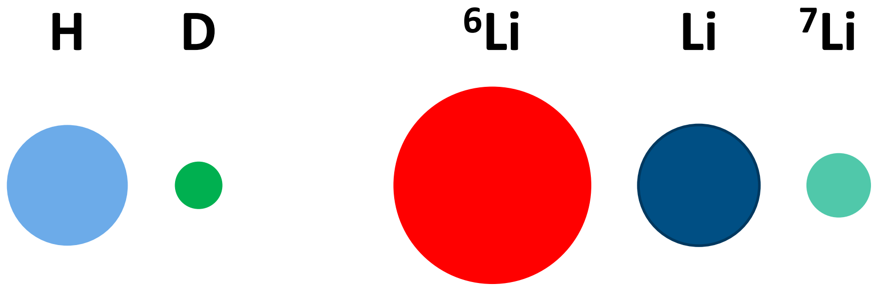

- dynamic imaging
- time resolved tomography
- diffraction contrast and polarized neutron imaging
- quantitative data analysis

Outlook

- Instruments and Detector getting more optimised
  → Higher spatial and temporal resolution

- Similar length scale as X-rays (cm to µm)

Complementarity

X-rays
Information about structural changes

Neutrons
Information about the electrochemistry

- Useful in a width field of Energy System:
  - Li Batteries
  - Fuel Cells
  - Electrolysers
  - H-Storage

Thank You

For Your Attention!

HZB Helmholtz Zentrum Berlin

HZB BESSY

UCL

electrochemical innovation lab

NEUTRONS FOR SCIENCE®

ZIB ZUSE INSTITUTE BERLIN

Science & Technology Facilities Council ISIS

UGA Université Grenoble Alpes

Oxford Neutron School 2024